Accepted Manuscript

Discovery of novel anti-angiogenesis agents. Part 7: Multitarget inhibitors of VEGFR-2, TIE-2 and EphB4

Chuansheng Li, Yuanyuan Shan, Ying Sun, Ru Si, Liyuan Liang, Xiaoyan Pan, Binghe Wang, Jie Zhang

PII: S0223-5234(17)30822-X

DOI: 10.1016/j.ejmech.2017.10.030

Reference: EJMECH 9822

To appear in: *European Journal of Medicinal Chemistry*

Received Date: 14 June 2017

Revised Date: 3 August 2017

Accepted Date: 10 October 2017

Please cite this article as: C. Li, Y. Shan, Y. Sun, R. Si, L. Liang, X. Pan, B. Wang, J. Zhang, Discovery of novel anti-angiogenesis agents. Part 7: Multitarget inhibitors of VEGFR-2, TIE-2 and EphB4, *European Journal of Medicinal Chemistry* (2017), doi: 10.1016/j.ejmech.2017.10.030.

Discovery of novel anti-angiogenesis agents. Part 7: Multitarget inhibitors of VEGFR-2, TIE-2 and EphB4

Chuansheng Li[a,†], Yuanyuan Shan[b,†], Ying Sun[a], Ru Si[a], Liyuan Liang[a], Xiaoyan Pan[a], Binghe Wang[c], Jie Zhang[a,*]

[a]*School of Pharmacy, Health Science Center, Xi'an Jiaotong University, No. 76, Yanta West Road, Xi'an, 710061, China*

[b]*Department of Pharmacy, The First Affiliated Hospital of Xi'an Jiaotong University, Xi'an, 710061, China*

[c]*Department of Chemistry and Center for Diagnostics and Therapeutics, Georgia State University, Atlanta, Georgia 30303, United States*

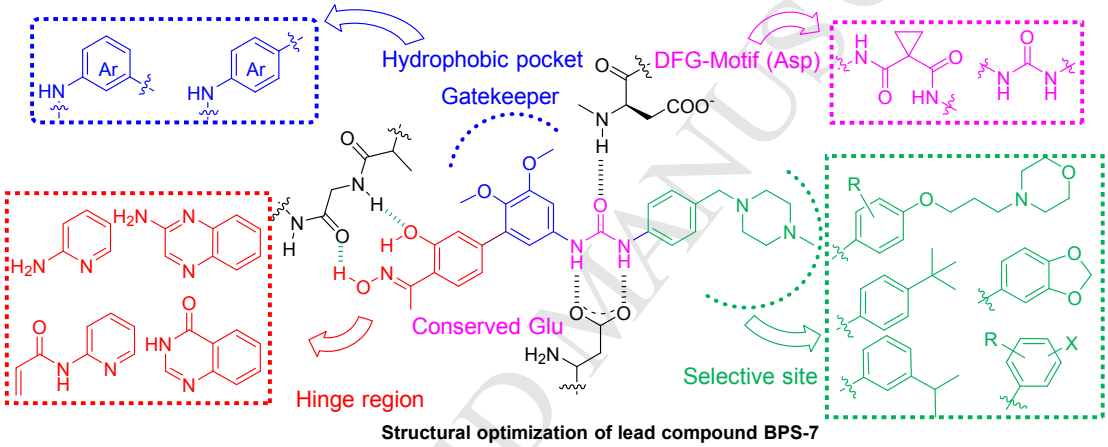

Structural optimization of lead compound BPS-7

As a continuation to our previous research, several triple RTK inhibitors of VEGFR-2, Tie-2 and EphB4 were designed and synthesized as novel anti-angiogenesis agents.

* Corresponding author. Tel/Fax: +86-29-82655451; E-mail: zhj8623@xjtu.edu.cn (Jie Zhang).

† Both authors contributed equally to this work and should be regarded as joint first authors.

European Journal of Medicinal Chemistry

journal homepage: http://www.elsevier.com/locate/ejmech

Discovery of novel anti-angiogenesis agents. Part 7: Multitarget inhibitors of VEGFR-2, TIE-2 and EphB4

Chuansheng Li[a,†], Yuanyuan Shan[b,†], Ying Sun[a], Ru Si[a], Liyuan Liang[a], Xiaoyan Pan[a], Binghe Wang[c], Jie Zhang[a,*]

[a]*School of Pharmacy, Health Science Center, Xi'an Jiaotong University, No. 76, Yanta West Road, Xi'an, 710061, China*
[b]*Department of Pharmacy, The First Affiliated Hospital of Xi'an Jiaotong University, Xi'an, 710061, China*
[c]*Department of Chemistry and Center for Diagnostics and Therapeutics, Georgia State University, Atlanta, Georgia 30303, United States*

ARTICLE INFO

Article history:
Received
Received in revised form
Accepted
Available online

Keywords:
Anti-angiogenesis Agents
Triple Inhibitors
Angiogenic RTKs
Hinge-binding group
N-(pyridin-2-yl)acrylamide

ABSTRACT

Herein, we embarked on a structural optimization campaign aiming at the discovery of second generation anti-angiogenesis agents with our previously reported BPS-7 as lead compound. A library of 27 compounds has been afforded based on the highly conserved ATP-binding pocket of VEGFR-2, Tie-2, and EphB4. Several title compounds exhibited simultaneous inhibitory effects against three angiogenic RTKs. These compounds with a 'triplet' inhibition profile have been identified as novel anti-angiogenic and anticancer agents. The representative VDAU11 displayed prominent anti-angiogenic and anticancer potency and could be considered as a candidate for further optimization. These results indicate that *N*-(pyridin-2-yl)acrylamide could serve as a novel hinge-binding group of triple inhibitors.

* Corresponding author. Tel/Fax: +86-29-82655451; E-mail: zhj8623@xjtu.edu.cn (Jie Zhang).
† Both authors contributed equally to this work and should be regarded as joint first authors.

1. Introduction

Angiogenesis plays a significant role in the pathogenesis of a variety of disorders including cancer, proliferative retinopathies, rheumatoid arthritis or psoriasis [1]. In addition, angiogenesis is widely identified as a crucial factor in metastasis, which is a major contributor to cancer-related death. Therefore, inhibition of angiogenesis has been considered as an attractive strategy for the treatment of cancers. Many anti-angiogenesis agents have been under clinical trial, or approved for clinical use. On the opposite, many limitations have been disclosed including resistance, enhancing hypoxia, and reducing delivery of drugs. Intracellular signals for angiogenesis including cell growth, proliferation, migration, and survival are frequently triggered by receptor tyrosine kinases (RTKs). Cancer cells secrete various RTKs involved in the process of angiogenesis [2]. Interaction of vascular endothelial growth factors (VEGFs) and its receptor (VEGF Receptor-2, VEGFR-2) promotes epithelial cell (EC) survival, proliferation, and migration [3]. Angiopoietin (Ang) and its receptor (tyrosine kinase with Ig and epidermal growth factor homology domain-2, Tie-2) are essential for vessel maturation, stabilization, and remodeling of vasculature [4]. Activation of erythropoietin-producing hepatoma receptor B4 (EphB4) by its membrane-associated ligand, ephrinB2, is critical for vessel maturation, remodeling, and stabilization [5].

The possibility of inhibiting angiogenic RTK has led to development of specific RTK inhibitors as anti-angiogenesis and anticancer agents. However, acquired resistance caused by compensatory activation of multiple RTKs limit the benefit of these drugs [6]. It has been revealed that simultaneous inhibition and combinatorial targeting of multiple pro-angiogenic RTKs have been recognized as valuable strategies to maximize the therapeutic potential [7]. There are several small molecular multi-target RTK inhibitors in clinical trials as anti-angiogenesis agents. Five drugs with different inhibition profile against angiogenic RTKs have been approved including Sorafenib (Nexavar, Bayer) [8], Regorafenib (Stivarga, Bayer), Linifanib (ABT-869, Abbott) [9], Vandetanib (Caprelsa, AstraZeneca) [10], and Cabozantinib (Cabometyx, Exelixis) [11] (**Figure 1**). Encouraged by previous results, we described here the discovery of a series of multiplex inhibitors of VEGFR-2/EphB4/TIE-2 as novel anti-angiogenesis agents.

*<Insert **Figure 1** here>*

To the best of our knowledge, all the three RTKs contain a highly conserved catalytic site binding with ATP. The catalytic domains and ATP-binding site in the active conformation of these RTKs are notably similar. Moreover, it is reasonable to assume that all the ATP-competitive RTKIs with anti-angiogenesis potency bind to the ATP binding site of RTKs. Overlay of the crystal structures of the three RTKs is depicted in **Figure 2**. Structural alignment indicated that there was no significant difference. The RMSD values for them are 0.849 Å, 0.725 Å, and 0.706 Å, respectively. As the structures display a similar two-lobed architecture and highly similar to each other, we believe that the similarity of kinase domains makes the multiplex inhibitors a feasible drug discovery strategy.

*<Insert **Figure 2** here>*

In our previous research, we have focused on the discovery of novel VEGFR-2 inhibitors as anti-angiogenesis agents. Numbers of biphenyl-aryl urea incorporated with salicylaldoxime including BPS-7 have been developed as potent and selective VEGFR-2 inhibitors (**Figure 3**) [12-17]. Based on conserved active sites of three angiogenic RTKs (VEGFR-2, Tie-2, and EphB4) and similar interaction conformation of inhibitors with them, we propose that the rational design of triple inhibitors of VEGFR-2/Tie-2/EphB4 is a promising strategy for discovery of anti-angiogenesis agents. Extensive structural optimization was conducted to expand structural diversity and improve activity using following strategies (**Figure 3**): (i) We explored various aromatic-heterocyclics as hinge binding group (HBG) via core-refining approach. Pyridin-2-amine, *N*-(pyridin-2-yl)acrylamide, quinoxalin-2-amine, and quinazolin-4(3*H*)-one were introduced as novel HBG.

These heterocyclics bearing various hydrogen bond donors or acceptors could retain the essential hydrogen bonds with hinge region of RTKs. We supposed that these groups might simultaneously form hydrogen bonds with hinge region of three RTKs and therefore provide an opportunity to improve affinity with receptors; (ii) The two methoxyl groups on biphenyl were removed to reduce the steric hindrance of ligands binding with receptors. In addition, we investigated the effect of position of urea on their biological activity; (iii) Inspired by the classic bioisosteric paradigm, urea moiety was replaced with cyclopropane-1,1-dicarboxamide which bears more hydrogen bond donors and acceptors; (iv) Aniline bearing halogen substituents is beneficial for antitumor potency and halogen could enhance the persistence and lipid solubility [18]. Therefore, various anilines bearing halogen were incorporated to develop novel anti-angiogenesis agents. In addition, other anilines containing morpholine side chain, *tert*-butyl, alkynyl, or benzo[d][1,3]dioxole were also incorporated at terminal as fragments interacting with active site.

<*Insert* ***Figure 3*** *here*>

Herein, we performed the design, synthesis, and biological evaluation of three classes of triple inhibitors of VEGFR-2, Tie-2, and EphB4. Several biphenyl-aryl ureas incorporated with quinazolin-4(3*H*)-one displayed promising anti-angiogenic and anti-cancer potency. The representative compound VDAU11 could be considered as a promising lead compound for further structural optimization.

2. Results and discussion

2.1 Chemistry

The synthetic routes of title compounds were illustrated in **Scheme 1**-**3**. The synthetic route for cyclopropyl-malonic amide derivatives **CPMA1-11** was outlined in **Scheme 1**. Commercially available 5-bromo-2-fluorobenzaldehyde **1** was converted to 6-bromoaminoquinazoline **2** by treatment with guanidine carbonate in *N*,*N*-dimethylacetamide. The critical intermediate **2** was subsequently converted to **4** through Pd-catalyzed Suzuki coupling with 4-aminophenylboronic acid **3**. Coupling of 1-cyclopropanedicarboxylate **5** with substituted aniline **6** in the presence of thionyl chloride gave intermediates **7**. Finally, treatment of intermediates **7** with **4** in the presence of triethylamine and 1-[Bis(dimethylamino)methylene]-1*H*-1,2,3-triazolo [4,5-b]pyridinium 3-oxide hexafluorophosphate (HATU) afforded cyclopropyl-malonic amide derivatives **CPMA1-11**. The synthetic route for title compounds **VDAU1-11** is described in **Scheme 2**. Firstly, the key intermediates **9** were prepared from commercial available 4-(4,4,5,5-tetramethyl-1,3,2-dioxaborolan-2-yl)aniline **8**. Various substituted anilines were treated with BTC in anhydrous CH_2Cl_2 to yield isocyanate, followed by reacting with **8** to generate diaryl ureas **9**. $Pd(PPh_3)_4$catalyzed Suzuki reaction of diaryl ureas **9** with 2-amino-5-bromopyridine **10** in presence of cesium carbonate in acetonitrile/H_2O afforded the key intermediates **11**. Finally, the title compounds **VDAU1-11** were prepared through acylation with acryloyl chloride. The synthetic route of quinazolinone diaryl urea derivatives **QZAU1-5** is shown in **Scheme 3**. 2-Amino-5-bromobenzoic acid **12** was converted to intermediate **13** by cyclization with formamide under atmospheric microwave heating at 150°C. The coupling substrates **15** were obtained by condensation of amino-boronate **14** with various isocyanates, which were prepared from reaction of anilines with BTC. Subsequently, the title commands **QZAU1-5** were prepared from **13** and **15** by Suzuki coupling reaction. All the title compounds characterized by ^{1}H-NMR, ^{13}C-NMR, high resolution mass spectrum (HRMS), and melting point analysis and their purity were above 95% determined by LC-MS (**Supplementary Material**).

<*Insert* ***Scheme 1-3*** *here*>

2.2 RTK inhibitory activity

All the title compounds were evaluated for their inhibitory potency against VEGFR-2, TIE-2 and EphB4 with sorafenib as a positive control (**Table 1**-**3**). Tyrosine kinase inhibition were tested by luminescent ADP-Glo^{TM} assay. We began our exploration with optimization of urea core

and hinge binding group of BPS-7. Firstly, we investigated the replacement of urea unit with cyclopropane-1,1-dicarboxamide. Meanwhile, quinazolin-2-amine was incorporated as a novel hinge binding group. The results in **Table 1** showed that the majority of these compounds exhibited significantly decreased RTK inhibitory activities compared with lead compound except for CPMA1, CPMA5 and CPMA7. These results indicated that the urea moiety was critical and the replacement of urea resulted in a significant loss in RTK inhibition. In addition, quinazolin-2-amine was not a favorable hinge binding group for multi-target RTK inhibitors. Compound CPMA7 bearing 3,4-difluoroaniline exhibited the highest RTKs inhibitory activities with IC_{50} values of 21.37 nM (VEGFR-2), 14.49 nM (Tie-2), and 37.78 nM (EphB4), respectively. The results suggested that 3,4-difluoro substituents led to improvement in simultaneous inhibition of VEGFR-2, Tie-2, and EphB4.

<*Insert* ***Table 1*** *here*>

Inspired by the above investigation, *N*-(pyridin-2-yl)acrylamide was introduced onto diaryl urea scaffold as novel hinge binding group (**Table 2**). The activity data indicated that two title compounds (VDAU2, VDAU11,) exhibited simultaneous and potent inhibition against VEGFR-2, Tie-2, and EphB4. In particular, VDAU11 bearing 3-chlorine substituent at terminal aniline was the most potent multi-target RTK inhibitor with IC_{50} values of 2.35 nM (VEGFR-2), 5.63 nM (Tie-2), and 3.87 nM (EphB4), respectively. The results suggested that *N*-(pyridin-2-yl)acrylamide could serve as a novel and potent hinge binding group for triple inhibitors of VEGFR-2, Tie-2, and EphB4.

<*Insert* ***Table 2*** *here*>

Encouraged by the promising multiple RTK inhibition of diaryl ureas, we chose to continue our structural optimization keeping urea unit constant. Quinazolin-4(3*H*)-one was incorporated onto diaryl urea core as a novel hinge binding group of multi-target inhibitors (**Table 3**). The results indicated that *meta*-substitution of quinazolin-4(3*H*)-one on diaryl ureas were favorable for angiogenic RTK inhibition. In addition, two title compounds (QZAU4, QZAU5) displayed simultaneously inhibitory potency against VEGFR-2, Tie-2, and EphB4. In particular, QZAU4 bearing 3,4-difluoroaniline was the most potent multi-target RTKs inhibitors with IC_{50} values of 28.95 nM (VEGFR-2), 16.55 nM (Tie-2), and 38.52 nM (EphB4), respectively. This study identified that quinazolin-4(3*H*)-one was a promising hinge binding group for triple inhibitors of VEGFR-2, Tie-2, and EphB4 as anti-angiogenesis and anticancer agents.

<*Insert* ***Table 3*** *here*>

2.3. RTK selectivity assay

In order to determine the RTK selectivity profile of the most potent compounds, VDAU11, a broad panel kinase screening was further conducted by evaluating the inhibition against other ten RTKs including VEGFR-1, VEGFR-3, EGFR, FGFR-1, FGFR-4, PDGFR-β, IGF1-R, B-Raf, c-Kit, and c-Met (**Figure 4** and **Table 4**). Besides VEGFR-2, Tie-2, and EphB4, VDAU11 displayed moderate inhibitory activity against FGFR-1 and PDGFR-β. Interestingly, they also exhibited potent inhibition against VEGFR-1, VEGFR-3, and B-Raf with IC_{50} values less than 50 nM. The results confirmed that these triple inhibitors exhibited good selectivity on VEGFR-2/TIE-2/EphB4 relative to other RTKs including EGFR, FGFR-1, FGFR-4, IGF1-R, c-Kit, and c-Met.

<*Insert* ***Figure 4*** *here*>

<*Insert* ***Table 4*** *here*>

2.4. Cell growth inhibition

In order to determine the potential anti-angiogenic effect of these triple inhibitors, we evaluate the inhibition of title compounds on HUVECs (EA.hy926) viability using cell counting kit-8 (CCK-8) method [19]. As shown in **Table 5**, majority of them displayed moderate to high antiproliferative activities with IC_{50} values ranging from 3.53 μM to 197.44 μM. Three compounds (CPMA5, CPMA7, and VDAU11) exhibited potent inhibition against the growth of human vascular endothelial cell with IC_{50} values less than 10 μM. Particularly, compound VDAU11 with the most potent RTK inhibitory activities exhibited

the highest cell growth inhibition with IC_{50} value of 3.53 μM. This compound represents the promising candidate with a "triplet" inhibition profile as well as anti-angiogenesis potency. It might not only inhibit the process of angiogenesis, but also prevent the occurrence of resistance.

*<Insert **Table 5** here>*

2.5. Anti-proliferative activity against cancer cells

RTKs and angiogenesis played critical role in the proliferation of various cancers cells and RTK inhibition generally translated well into anti-proliferation of cancer cells. In this regard, in order to investigate the potential anticancer potency of these multi-target RTK inhibitors, the most potent VDAU11 was selected to examine its anti-proliferative activity against fifteen cancer cells including human hepatic cancer cell lines (97h, BEL-7402, Hep3B,), human breast cancer cell lines (MCF-7, ZR-75-30), human pancreatic cancerous cell lines (PANC-1), human lung cancer cell (A549), human colon carcinoma cell line (LOVO), and human cervical cancer cell line (HeLa). Highly consistent with the RTK inhibition, we are pleased to find that VDAU11 significantly inhibited growth of all nine cancer cell lines with IC_{50} values ranging from 2.70 μM to 22.93 μM (**Figure 5**). It displayed comparable anti-proliferative potency with sorafenib. The highest activity for VDAU11 were found in human breast cancer cell lines (MCF-7) and human lung cancer cell (A549) with IC_{50} values of 2.70 μM. In summary, VDAU11 displayed significant anti-proliferative activity against a broad spectrum of cancer cell lines.

*<Insert **Figure 5** here>*

2.6 Molecular docking study

For further structural optimization and investigation of the potential binding mode, molecular modeling studies were performed using Sybyl-X (Version 2.0, Tripos Inc. St. Louis, MO). The most potent compound, VDAU11, was constructed and optimized using Powell's method with a Tripos force field. The molecular modeling was performed using Sybyl-X/Surflex-dock module, and the residues in a 5.0 Å radius around the natural ligand of VEGFR-2 (PDB ID: 4ASD), Tie-2 (PDB ID: 2P4I) and EphB4 (PDB ID: 2X9F) were selected as the active site. The binding mode of CDAU-2 with the ATP-pocket of VEGFR-2 (A), TIE-2 (B), EphB4 (C) were depicted in **Figure 6-8**. Favorable binding interactions of VDAU11 with the active site of VEGFR-2 included three hydrogen bonds (**Figure 6**): *N*-(pyridin-2-yl)acrylamide in VDAU11 forms one hydrogen bond with Cys 919 in the hinge region of VEGFR-2 with distance of 2.37 Å. In addition, the NH of urea formed one hydrogen bond with conserved Glu 885 for the bond length of 1.95 Å, while CO formed a hydrogen bond with Asp 1046 of DFG-motif with distance of 1.76 Å. As for TIE-2, the binding model was described in **Figure 7**. NH of acrylamide also formed a hydrogen bond with Ala 905 in hinge region of TIE-2 with the bond length of 1.92 Å. While the CO of acrylamide forms another hydrogen bond with Tyr 904 in hinge region with distances of 2.34 Å. As shown in **Figure 8**, *N*-(pyridin-2-yl)acrylamide in VDAU11 forms one hydrogen bond with Thr 693 in the hinge region of EphB4 with distance of 2.62 Å. *N*-(pyridin-2-yl)acrylamide could form one or two hydrogen bonds with hinge region of three angiogenic RTKs. These molecular docking results indicated that the *N*-(pyridin-2-yl)acrylamide is beneficial for affinity of inhibitors with VEGFR-2, TIE-2, and EphB4. It could be considered as novel hinge-binding group for further discovery of triple RTK inhibitors.

*<Insert **Figure 6-8** here>*

Molecular docking results provided a better understanding of VDAU11's interaction with three angiogenic RTKs. Our docking results might explain why VDAU11 displayed potent inhibitory activities against all three proteins. In addition, *N*-(pyridin-2-yl)acrylamide was beneficial for simultaneous inhibition of RTKs.

3. Conclusion

In summary, we described the triple inhibitors of VEGFR-2/TIE-2/EphB4 as potential anti-angiogenesis and anticancer agents. *N*-(pyridin-2-yl)acrylamide was firstly introduced to diaryl urea core as hinge-binding group of triple inhibitors. The biological results indicated that

VDAU11 displayed stimultaneous inhibition of VEGFR-2, TIE-2 and EphB4 and is marginally better than the positive control (Sorafenib) in two of three inhibitors. Meanwhile, it displayed the most potent antiproliferative activity against human vascular endothelial cell (EA. hy926). In addition, VDAU11 exhibited comparable anticancer activity compared with sorafenib. Several title compounds (CPMA1, CPMA5, CPMA6, CPMA7, VDAU2, VDAU11, QZAU4, and QZAU5) exhibited simultaneous inhibition against VEGFR-2, TIE-2 and EphB4, three angiogenic RTK. They might be considered as novel lead compound for further discovery of triple RTK inhibitors as anti-angiogenesis and anticancer agents. They might not only inhibit the process of angiogenesis, but also prevent drug resistance. Moreover, biological evaluation and molecular docking indicated that *N*-(pyridin-2-yl)acrylamide was beneficial for potency of these triple inhibitors. It could be considered as a novel hinge-binding group for further discovery of novel anti-angiogenesis agents.

4. Experimental section

4.1. Chemistry: General procedure

Reagents and solvents are purified according to the standard procedure. The reactions except those in aqueous are performed by standard techniques for the exclusion of moisture. Reactions are monitored by thin layer chromatography (TLC) on 0.25-mm silica gel plates (60GF-254) and visualized with UV light. Melting points are determined on electrothermal melting point apparatus and are uncorrected. ^{1}H NMR and ^{13}C NMR spectra are measured at 400 MHz on a Bruker Advance AC 400 instrument with TMS as an internal standard. High resolution mass spectra (HRMS) are obtained on a Shimadzu LCMS-IF-TOF instrument.

4.2. General procedure for the synthesis of cyclopropyl-malonic amide derivatives CPMA1-11.

4.2.1. 6-Bromoquinazolin-2-amine (2).

2-Fluoro-5-bromobenzaldehyde (10 g, 49.2 mmol) and bisguanidinium carbonate (13.3 g, 74 mmol) were dissolved in *N*,*N*-dimethylacetamide (50 mL). The resulting mixture was heated to reflux and stirred for 5 h. After cooling to room temperature, 120 mL water was added and the reaction mixture was allowed to stir for another 2 h at room temperature. The product was collected by filtration and dried under vacuum to afford 6-bromo-2-quinazolinamine (**2**) (5.0 g, 60%).

4.2.2. 7-(4-Aminophenyl)- 2-quinazolinamine (4).

$Pd(PPh_3)_4$ (1.03 g, 0.89 mmol) was added to a degassed solution of 4-aminophenyl boronic acid (1.54 g, 8.9 mmol), K_2CO_3 (2.8 g, 26.7 mmol), 6-bromo-2-quinazolinamine (**2**) (2.0 g, 8.9 mmol) in 120 mL 1,4-dioxane and 40 mL water. The reaction mixture was heated at 100°C in an oil bath and stirred under nitrogen for 24 h. The mixture was dissolved in H_2O and then extracted with ethyl acetate (30 mL×3). The combined organic layer was washed with brine, dried over Na_2SO_4, filtered, and concentrated *in vacuo* to give the crude product, which was isolated by silica gel flash chromatography (PE/AcOEt =3:1)to yield the key intermediate **4** (0.8 g, yield 28%).

4.2.3. 1-((3,5-dimethylphenyl)carbamoyl)cyclopropane carboxylic acid (7).

1,1-Cyclopropanedicarboxylic acid (**5**) (12.0 g, 15.4 mmol) was dissolved in anhydrous THF (50 mL). Then triethanolamine (2.0 mL,13.9mmol) was added to the mixture and the mixture was stirred on the ice-bath for 30 min. $SOCl_2$ (1.2 mL, 16.66 mmol) was then added. Stirring was continued for 2h, a solution of 3,5-dimethylaniline **6** (3.6 g, 15.4 mmol) in anhydrous THF (10 mL) was added and continued stirring for 2h, after that, the ice bath was removed, and the mixture was stirred at room temperature overnight. After the completion of the reaction, the mixture was filtered and concentrated *in vacuo*. The residues was purified by silica gel flash chromatography (PE/AcOEt=5:1) to yield **7** as white solid (0.8 g, 30.7%).

4.2.4. N-(4-(2-aminoquinazolin-7-yl)phenyl)-N-(3-bromo-5-(trifluoromethyl)phenyl)cyclopropane-1,1-dicarboxamide (CPMA1).

To a mixture of **7** (0.24 g, 0.70 mmol) and 4 (0.38 g, 0.70 mmol) dissolved in 5 mL of THF in ice-bath, HATU (0.48 mg, 1.26 mmol) was added. After stirring for 30 min, triethanolamine (0.10 mL, 0.56 mmol) was dropped. The

reaction was warmed to the room temperature and stirred overnight. After the completion of the reaction, the mixture was filtered and the filtrate distilled by rotary evaporation to remove THF. Water (50 mL) was added and the product was extracted with AcOEt (30 mL×3), washed with water, and dried over Na_2SO_4. After filtration and concentration *in vacuo*, the residue was purified by silica gel flash chromatography (PE/AcOEt = 3:1) to afford **CPMA1** as white solid. HRMS *m/z* calcd for $C_{26}H_{19}BrF_3N_5O_2$ ($[M+H]^+$) 570.0674, found570.0654.m.p.=234-236°C,^{1}H NMR (400 MHz, DMSO) δ 11.49 (s, 1H), 9.74 (s, 1H), 9.16 (s, 1H), 8.44 (s, 1H), 8.12 (d, *J* = 2.0 Hz, 1H), 8.05 (m,1H), 7.76 (d, *J* = 8.8 Hz, 2H), 7.72 (d, *J* = 8.8 Hz, 2H), 7.50 (d, *J* = 8.8 Hz, 1H), 7.43 (s, 2H), 6.90 (s, 2H), 1.76 (m, 2H), 1.63 (m, 2H).^{13}C NMR (101 MHz, DMSO) δ 170.78, 168.99, 163.07, 161.35, 151.65, 138.40, 137.77, 135.57, 133.37, 133.17, 132.98, 127.94, 126.92, 126.04, 125.57, 125.20, 123.75, 122.29, 121.78, 120.46, 120.15, 29.84, 18.16.

Compounds **CPMA2-11** were prepared from the key intermediate **4** and **7** with a similar procedure as described for compound **CPMA1**.

4.2.5. N-(4-(2-aminoquinazolin-7-yl)phenyl)-N-(3-bromo-5-(trifluoromethoxy)phenyl)cyclopropane-1,1-dicarboxamide (CPMA2).

HRMS *m/z* calcd for $C_{26}H_{19}BrF_3N_5O_3$ ($[M+H]^+$) 586.0623, found 586.0676. m.p.=224-225°C, ^{1}H NMR (400 MHz, DMSO) δ 11.31 (s, 1H), 9.80 (s, 1H), 9.16 (s, 1H), 8.13 (m, 2H), 8.05 (m, 1H), 7.76 (m, 2H), 7.74-7.69 (m, 3H), 7.63 (m, 1H), 7.49 (d, *J* = 8.8 Hz, 1H), 6.92 (s, 2H), 1.74 (m, 2H), 1.66-1.57 (m, 2H).^{13}C NMR (101 MHz, DMSO) δ 170.68, 168.86, 163.09, 161.34, 151.64, 139.76, 137.82, 135.51, 133.37, 133.18, 131.53, 131.15, 126.92, 125.56, 125.47, 125.19, 124.93, 122.18, 120.14, 116.09, 29.90, 17.96.

4.2.6. N-(4-(2-aminoquinazolin-7-yl)phenyl)-N-(2-bromo-5-(trifluoromethoxy)phenyl)cyclopropane-1,1-dicarboxamide (CPMA3).

HRMS *m/z* calcd for $C_{26}H_{19}BrF_3N_5O_3$ ($[M+H]^+$) 586.0623, found 586.0675. m.p.=212-214°C, ^{1}H NMR (400 MHz, DMSO) δ 11.31 (s, 1H), 9.79 (s, 1H), 9.17 (s, 1H), 8.12 (m, 2H), 8.05 (m, 2.1 Hz, 1H), 7.74 (d, *J* = 5.4 Hz, 4H), 7.70 (s, 1H), 7.63 (m, 1H), 7.50 (d, *J* = 8.8 Hz, 1H), 6.91 (s, 2H), 1.76-1.72 (m, 2H), 1.62 (m, 2H).^{13}C NMR (101 MHz, DMSO) δ 170.70, 168.86, 163.07, 161.35, 151.65, 139.75, 137.81, 135.53, 133.39, 133.17, 131.50, 131.15, 126.92, 125.57, 125.44, 125.19, 124.89, 122.20, 121.80, 120.15, 116.06, 29.88, 17.98.

4.2.7. N-(4-(2-aminoquinazolin-7-yl)phenyl)-N-(5-bromo-2-(trifluoromethoxy)phenyl)cyclopropane-1,1-dicarboxamide (CPMA4).

HRMS *m/z* calcd for $C_{26}H_{19}BrF_3N_5O_3$ ($[M+H]^+$) 586.0623, found 586.0674. m.p.=239-240°C, ^{1}H NMR (400 MHz, DMSO) δ 11.48 (s, 1H), 9.74 (s, 1H), 9.16 (s, 1H), 8.44 (d, *J* = 0.8 Hz, 1H), 8.12 (d, *J* = 2.0 Hz, 1H), 8.05 (m, 1H), 7.76 (d, *J* = 8.9 Hz, 2H), 7.72 (d, *J* = 8.9 Hz, 2H), 7.50 (d, *J* = 8.8 Hz, 1H), 7.44 (s, 2H), 6.90 (s, 2H), 1.76 (m, 2H), 1.63 (m, 2H).^{13}C NMR (101 MHz, DMSO) δ 170.78, 168.99, 163.07, 161.35, 151.65, 138.41, 137.77, 135.57, 133.37, 133.17, 132.98, 127.95, 126.92, 126.04, 125.57, 125.20, 123.75, 122.29, 121.78, 120.46, 120.15, 29.85, 18.16.

4.2.8. N-(4-(2-aminoquinazolin-7-yl)phenyl)-N-(2-bromo-5-(trifluoromethoxy)phenyl)cyclopropane-1,1-dicarboxamide (CPMA5).

HRMS *m/z* calcd for $C_{26}H_{19}BrF_3N_5O_3$ ($[M+H]^+$) 586.0623, found 586.0673. m.p.=191-192°C, ^{1}H NMR (400 MHz, DMSO) δ 9.17 (s, 1H), 8.19 (d, *J* = 2.0 Hz, 1H), 8.10 (d, *J* = 1.8 Hz, 1H), 8.04 (m, 1H), 7.81 (d, *J* = 8.8 Hz, 1H), 7.78-7.69 (m, 4H), 7.50 (d, *J* = 8.8 Hz, 1H), 7.12 (d, *J* = 8.0 Hz, 1H), 6.90 (s, 2H), 1.72 (d, *J* = 10.8 Hz, 2H), 1.66 (s, 2H).^{13}C NMR (101 MHz, DMSO) δ 170.49, 169.30, 163.07, 161.34, 151.65, 148.01, 137.84, 135.55, 134.31, 133.45, 133.19, 126.97, 125.59, 125.18, 122.40, 121.69, 120.15, 119.14, 116.31, 113.51, 60.21, 30.05, 18.16.

4.2.9. N-(4-(2-aminoquinazolin-7-yl)phenyl)-N-(2,4-dichlorophenyl)cyclopropane-1,1-dicarboxamide (CPMA6).

HRMS *m/z* calcd for $C_{25}H_{19}Cl_2N_5O_2$ ($[M+H]^+$) 492.0916, found 492.0967. m.p.=261-263°C, ^{1}H NMR (400 MHz,

DMSO) δ 10.99 (s, 1H), 9.93 (s, 1H), 9.17 (s, 1H), 8.09 (d, *J* = 8.7 Hz, 2H), 8.04 (d, *J* = 8.8 Hz, 1H), 7.74 (m, 4H), 7.70-7.68 (m, 1H), 7.50 (d, *J* = 8.7 Hz, 1H), 7.44 (m, 1H), 6.90 (s, 2H), 1.71 (s, 2H), 1.64 (s, 2H).^{13}C NMR (101 MHz, DMSO) δ 170.35, 168.99, 163.07, 161.34, 151.65, 137.86, 135.53, 134.60, 133.44, 133.19, 129.23, 129.20, 128.18, 126.99, 126.27, 125.68, 125.59, 125.56, 125.17, 122.23, 120.15, 30.07, 17.86.

4.2.10. N-(4-(2-aminoquinazolin-7-yl)phenyl)-N-(3,4-difluorophenyl)cyclopropane-1,1-dicarboxamide (CPMA7).

HRMS *m/z* calcd for $C_{25}H_{19}F_2N_5O_2$ ([M+H]$^+$) 460.1507, found 460.1558. m.p.=263-266°C, ^{1}H NMR (400 MHz, DMSO) δ 10.24 (s, 1H), 10.11 (s, 1H), 9.16 (s, 1H), 8.09 (d, *J* = 2.0 Hz, 1H), 8.03 (m, 1H), 7.86-7.80 (m, 1H), 7.76 (d, *J* = 8.9 Hz, 2H), 7.74-7.70 (m, 2H), 7.49 (d, *J* = 8.8 Hz, 1H), 7.39 (m, 2H), 6.89 (s, 2H), 1.50 (s, 2H), 1.48 (s, 2H).^{13}C NMR (101 MHz, DMSO) δ 168.86, 168.34, 163.06, 161.30, 151.56, 138.71, 136.48, 136.39, 134.84, 133.53, 133.16, 126.90, 125.55, 125.01, 121.28, 120.16, 117.68, 117.51, 117.19, 110.04, 109.82, 32.32, 15.90.

4.2.11. N-(4-(2-aminoquinazolin-7-yl)phenyl)-N-(3,4-dichlorophenyl)cyclopropane-1,1-dicarboxamide (CPMA8).

HRMS *m/z* calcd for $C_{25}H_{19}Cl_2N_5O_2$ ([M+H]$^+$) 492.0916, found 492.0924. m.p.=253-254°C, ^{1}H NMR (400 MHz, DMSO) δ 10.32 (s, 1H), 10.11 (s, 1H), 9.17 (s, 1H), 8.09 (d, *J* = 2.0 Hz, 1H), 8.06 (d, *J* = 2.1 Hz, 1H), 8.03 (m, 1H), 7.77 (d, *J* = 8.8 Hz, 2H), 7.71 (d, *J* = 8.8 Hz, 2H), 7.60 (m, 1H), 7.56 (d, *J* = 8.8 Hz, 1H), 7.49 (d, *J* = 8.8 Hz, 1H), 6.90 (s, 2H), 1.52 (d, *J* = 10.2 Hz, 2H), 1.48 (d, *J* = 10.1 Hz, 2H).^{13}C NMR (101 MHz, DMSO) δ 169.01, 168.23, 163.05, 161.32, 151.58, 139.57, 138.73, 134.86, 133.54, 133.15, 131.19, 130.84, 126.90, 125.56, 125.40, 125.00, 122.08, 121.29, 120.75, 120.17, 32.49, 15.97.

4.2.12. N-(4-(2-aminoquinazolin-7-yl)phenyl)-N-(3,5-bis(trifluoromethyl)phenyl)cyclopropane-1,1-dicarboxamide (CPMA9).

HRMS *m/z* calcd for $C_{27}H_{19}F_6N_5O_2$ ([M+H]$^+$) 560.1443, found 560.1492. m.p.=218-219°C, ^{1}H NMR (400 MHz, DMSO) δ 10.68 (s, 1H), 10.16 (s, 1H), 9.17 (s, 1H), 8.39 (s, 2H), 8.09 (d, *J* = 1.9 Hz, 1H), 8.03 (m, 1H), 7.78 (d, *J* = 8.6 Hz, 3H), 7.72 (d, *J* = 8.8 Hz, 2H), 7.50 (d, *J* = 8.8 Hz, 1H), 6.90 (s, 2H), 1.52 (s, 4H).^{13}C NMR (101 MHz, DMSO) δ 169.52, 167.79, 163.04, 161.32, 151.59, 141.47, 138.80, 134.86, 133.53, 133.14, 131.13, 130.81, 126.91, 125.56, 125.11, 124.99, 122.40, 121.20, 120.42, 120.16, 116.59, 32.82, 15.89.

4.2.13. N-(4-(2-aminoquinazolin-7-yl)phenyl)-N-(3-fluoro-4-(3-morpholinopropoxy)phenyl)cyclopropane-1,1-dicarboxamide (CPMA10).

HRMS *m/z* calcd for $C_{32}H_{33}FN_6O_4$ ([M+H]$^+$) 585.2547, found 585.2560. m.p.=213-214°C, ^{1}H NMR (400 MHz, DMSO) δ 10.17 (s, 1H), 10.02 (s, 1H), 9.16 (s, 1H), 8.09 (d, *J* = 2.0 Hz, 1H), 8.03 (m, 1H), 7.80 (s, 1H), 7.76 (d, *J* = 8.8 Hz, 2H), 7.72 (d, *J* = 8.9 Hz, 2H), 7.63 (m, 1H), 7.49 (d, *J* = 8.8 Hz, 1H), 7.31 (d, *J* = 8.9 Hz, 1H), 7.14 (m, 1H), 6.89 (s, 2H), 3.63-3.51 (m, 6H), 2.51 (m, 4H), 2.48 (s, 4H), 1.49 (s, 4H).^{13}C NMR (101 MHz, DMSO) δ 168.66, 168.55, 163.05, 161.31, 151.58, 142.72, 138.69, 134.83, 133.53, 133.16, 133.00, 132.90, 126.91, 125.56, 125.00, 121.25, 120.16, 116.94, 115.69, 109.64, 109.41, 67.44, 66.63, 57.38, 54.06, 32.00, 15.96.

4.2.14. N-(4-(2-aminoquinazolin-7-yl)phenyl)-N-(benzo[d][1,3]dioxol-5-yl)cyclopropane-1,1-dicarboxamide (CPMA11).

HRMS *m/z* calcd for $C_{26}H_{21}N_5O_4$ ([M+H]$^+$) 468.1627, found 468.1637. m.p.=283-285°C, ^{1}H NMR (400 MHz, DMSO) δ 10.21 (s, 1H), 9.91 (s, 1H), 9.17 (s, 1H), 8.09 (d, *J* = 1.8 Hz, 1H), 8.03 (m, 1H), 7.76 (d, *J* = 8.8 Hz, 2H), 7.72 (d, *J* = 8.8 Hz, 2H), 7.49 (d, *J* = 8.8 Hz, 1H), 7.32 (d, *J* = 1.5 Hz, 1H), 7.02 (m, 1H), 6.90 (s, 2H), 6.86 (d, *J* = 8.4 Hz, 1H), 6.00 (s, 2H), 1.49 (s, 4H).^{13}C NMR (101 MHz, DMSO) δ 168.71, 168.64, 163.05, 161.31, 151.58, 147.36, 143.76, 138.65, 134.84, 133.55, 133.47, 133.16, 126.92, 125.56, 125.01, 121.25, 120.17, 114.15, 108.24, 103.44, 101.44, 67.48, 31.78, 16.03.

4.2.15. General procedure for the synthesis of N-(pyridin-2-yl)acrylamidediaryl urea derivatives VDAU1-11.

4.2.16. 1-(4-(tert-butyl)phenyl)-3-(4-(4,4,5,5-tetramethyl-

1,3,2-dioxaborolan-2-yl)phenyl)urea (9).

Triphosgene (1.77 g, 6.03 mmol) was dissolved in anhydrous CH_2Cl_2 (30 mL) and the mixture was stirred on the ice-bath for 5 min. *Tert*-butyl-aniline (2.0 g, 13.4mmol) in anhydrous CH_2Cl_2 was added dropwise to the mixture and stirring was continued for 15 min. Then triethanolamine (2.2 mL, 16.1 mmol) diluted with CH_2Cl_2 (20 mL) was added onto the mixture. Stirring was continued for 15 min, a solution of triethanolamine (2.2 mL, 16.1 mmol) and 4-(4,4,5,5-tetramethyl-1,3,2-dioxaborolan-2-yl)aniline **8** (2.35 g, 10.72mmol) in anhydrous CH_2Cl_2 (30 mL) was added and continued stirring for 20 min. Subsequently, the ice bath was removed, and the mixture was reacted at room temperature overnight. After completion of the action, the reaction was quenched with dilute $NaHCO_3$. The organic layer was washed with water and brine, and dried over Na_2SO_4. After filtration and concentration *in vacuo*, the residue was purified by silica gel flash chromatography (PE/AcOEt = 3:1) yielding **10** as white solid (3.4 g, 64.4%).

4.2.17. 1-(4-(6-aminopyridin-3-yl)phenyl)-3-(4-(tert-butyl)phenyl)urea (11).

A flask charged with $Pd(PPh_3)_4$ (0.30 g, 0.26mmol), cesium carbonate (1.71 g, 5.26mmol), and intermediate **9** (1.00 g, 2.63mmol) and 2-amino-5-bromopyridine **10** (0.45 g, 2.63mmol) were flushed with nitrogen and suspended in 1,4-dioxane (90 mL) and water (30 mL). The mixture was then refluxed overnight under nitrogen. The hot suspension was filtered and the filtrate distilled by rotary evaporation to remove 1,4-dioxane. Water (50 mL) was added and the product was extracted with AcOEt (30 mL×3), washed with water, and dried over Na_2SO_4. After filtration and concentration *in vacuo*, the residue was purified by silica gel flash chromatography (PE/AcOEt = 3:1) affording **11** (0.56 g, 45.5%) as yellow solid.

4.2.18. N-(5-(4-(3-(4-(tert-butyl)phenyl)ureido)phenyl) pyridin-2-yl)acrylamide(VDAU1).

To a mixture of **11** (0.20 g, 0.55mmol) and triethanolamine (0.31 mL, 2.20 mmol) dissolved in 20 mL of THF in ice-bath. After stirring for 30 min, acryloyl chloride (0.11 mL, 1.33mmol) was dropped. The reaction was warmed to the room temperature and stirred overnight. After the completion of the reaction, the mixture was filtered and the filtrate distilled by rotary evaporation to remove THF. After filtration and concentration *in vacuo*, the residues was purified by silica gel flash chromatography (PE/AcOEt = 1:1) yielding **VDAU-1** as white solid (yield 21.7%), HRMS *m/z* calcd for $C_{25}H_{26}N_4O_2$ ($[M+H]^+$) 415.0156, found 415.0151. m.p.=180-182°C, ^{1}H NMR (400 MHz, DMSO) δ 10.82 (s, 1H), 8.78 (s, 1H), 8.66 (d, J = 2.4 Hz, 1H), 8.63 (s, 1H), 8.27 (d, J = 8.7 Hz, 1H), 8.10 (m, J = 8.7, 2.5 Hz, 1H), 7.66 (d, J = 8.7 Hz, 2H), 7.57 (d, J = 8.7 Hz, 2H), 7.39 (d, J = 8.7 Hz, 2H), 7.31 (d, J = 8.8 Hz, 2H), 6.64 (m, J = 17.0, 10.2 Hz, 1H), 6.33 (m, J = 17.0, 1.9 Hz, 1H), 5.83 – 5.77 (m, 1H), 1.27 (s, 10H). ^{13}C NMR (101 MHz, DMSO) δ 164.08, 152.97, 151.20, 145.80, 144.69, 140.09, 137.43, 135.98, 132.01, 131.60, 130.39, 128.20, 127.21, 125.87, 118.97, 118.60, 114.07, 34.37, 31.73.

The title compounds **VDAU2-11** were prepared from the key intermediate **11** and acryloyl chloride with a similar procedure as described for compounds **VDAU1**.

4.2.19. N-(5-(4-(3-(3-isopropylphenyl)ureido)phenyl) pyridin-2-yl)acrylamide (VDAU2).

White solid (yield 47.6%), HRMS *m/z* calcd for $C_{24}H_{24}N_4O_2$ ($[M+H]^+$) 400.1899, found 400.9911. m.p.=180-181°C, ^{1}H NMR (400 MHz, DMSO) δ 10.82 (s, 1H), 8.79 (s, 1H), 8.67 (d, J = 1.9 Hz, 2H), 8.28 (d, J = 8.6 Hz, 1H), 8.10 (m, J = 8.6, 2.3 Hz, 1H), 7.67 (d, J = 8.6 Hz, 2H), 7.58 (d, J = 8.6 Hz, 2H), 7.37 (s, 1H), 7.28 (d, J = 8.0 Hz, 1H), 7.20 (t, J = 7.8 Hz, 1H), 6.87 (d, J = 7.4 Hz, 1H), 6.65 (m, J = 17.0, 10.2 Hz, 1H), 6.38 – 6.29 (m, 1H), 5.84 – 5.76 (m, 1H), 2.93 – 2.78 (m, 1H), 1.19 (t, J = 11.5 Hz, 6H). ^{13}C NMR (101 MHz, DMSO) δ 164.09, 152.94, 151.22, 149.51, 145.81, 140.03, 135.99, 132.02, 131.60, 130.47, 129.16, 128.18, 127.21, 120.47, 119.04, 116.70, 116.36, 114.08, 33.97, 24.35.

4.2.20. N-(5-(4-(3-(4-chloro-3-(trifluoromethyl)phenyl) ureido)phenyl)pyridin-2-yl)acrylamide(VDAU3).

White solid (yield70.6%), HRMS *m/z* calcd for

$C_{22}H_{16}ClF_3N_4O_2$ ([M]$^+$) 460.0914, found 460.9700. m.p.=193-194°C, ^{1}H NMR (400 MHz, DMSO) δ 10.82 (s, 1H), 9.22 (s, 1H), 9.01 (s, 1H), 8.66 (d, J = 2.1 Hz, 1H), 8.28 (d, J = 8.7 Hz, 1H), 8.13 (d, J = 2.3 Hz, 1H), 8.10 (m, J = 8.7, 2.5 Hz, 1H), 7.68 (d, J = 8.7 Hz, 2H), 7.66 (d, J = 2.3 Hz, 1H), 7.63 (s, 1H), 7.59 (d, J = 8.7 Hz, 2H), 6.65 (m, J = 17.0, 10.2 Hz, 1H), 6.34 (m, J = 17.0, 1.8 Hz, 1H), 5.80 (m, J = 10.2, 1.8 Hz, 1H). ^{13}C NMR (101 MHz, DMSO) δ 164.09, 152.81, 151.29, 145.86, 139.78, 139.47, 136.05, 132.47, 132.00, 131.50, 131.01, 128.19, 127.23, 124.65, 123.57, 122.81, 119.48, 117.30, 114.07.

4.2.21. N-(5-(4-(3-(3-chloro-4-methylphenyl)ureido)phenyl) pyridin-2-yl)acrylamide (VDAU4).

White solid (yield 51.4%), HRMS *m/z* calcd for $C_{22}H_{19}ClN_4O_2$ ([M]$^+$) 406.1197, found 406.9234. m.p.=214-215°C, ^{1}H NMR (400 MHz, DMSO) δ 10.82 (s, 1H), 8.89 (s, 1H), 8.84 (s, 1H), 8.66 (d, J = 2.2 Hz, 1H), 8.27 (d, J = 8.7 Hz, 1H), 8.09 (m, J = 8.7, 2.5 Hz, 1H), 7.72 (d, J = 1.9 Hz, 1H), 7.67 (d, J = 8.7 Hz, 2H), 7.58 (d, J = 8.7 Hz, 2H), 7.25 (d, J = 8.4 Hz, 1H), 7.21 (m, J = 8.3, 2.0 Hz, 1H), 6.65 (m, J = 17.0, 10.2 Hz, 1H), 6.34 (m, J = 17.0, 1.8 Hz, 1H), 5.80 (m, J = 10.2, 1.8 Hz, 1H), 2.27 (s, 3H). ^{13}C NMR (101 MHz, DMSO) δ 164.09, 152.84, 151.24, 145.83, 139.80, 139.30, 136.00, 133.59, 132.01, 131.64, 131.55, 130.67, 128.76, 128.19, 127.21, 119.19, 118.64, 117.48, 114.07, 19.29.

4.2.22. N-(5-(4-(3-(3-fluorophenyl)ureido)phenyl)pyridin-2-yl)acrylamide (VDAU5).

White solid (yield 34.4%), HRMS *m/z* calcd for $C_{21}H_{17}FN_4O_2$ ([M]$^+$) 376.1336, found 376.9202. m.p.=199-201°C, ^{1}H NMR (400 MHz, DMSO) δ 10.82 (s, 1H), 8.99 (s, 1H), 8.93 (s, 1H), 8.66 (d, J = 2.1 Hz, 1H), 8.28 (d, J = 8.7 Hz, 1H), 8.10 (m, J = 8.7, 2.4 Hz, 1H), 7.68 (d, J = 8.7 Hz, 2H), 7.58 (d, J = 8.7 Hz, 2H), 7.55 – 7.49 (m, 1H), 7.32 (m, J = 15.2, 8.1 Hz, 1H), 7.15 (d, J = 8.1 Hz, 1H), 6.80 (m, J = 8.4, 2.1 Hz, 1H), 6.65 (m, J = 17.0, 10.2 Hz, 1H), 6.34 (m, J = 17.0, 1.8 Hz, 1H), 5.80 (m, J = 10.2, 1.8 Hz, 1H). ^{13}C NMR (101 MHz, DMSO) δ 164.10, 161.68, 152.80, 151.26, 145.84, 141.96, 139.71, 136.02, 132.02, 131.55, 130.78, 128.18, 127.23, 119.25, 114.46, 114.08, 108.55, 105.51, 105.25.

4.2.23. N-(5-(4-(3-(4-fluorophenyl)ureido)phenyl)pyridin-2-yl)acrylamide (VDAU6).

White solid (yield 15.6%), HRMS *m/z* calcd for $C_{21}H_{17}FN_4O_2$ ([M]$^+$) 376.1336, found 376.9213. m.p.=256-258°C, ^{1}H NMR (400 MHz, DMSO) δ 10.81 (s, 1H), 8.83 (s, 1H), 8.77 (s, 1H), 8.66 (d, J = 2.0 Hz, 1H), 8.27 (d, J = 8.7 Hz, 1H), 8.09 (m, J = 8.7, 2.4 Hz, 1H), 7.67 (d, J = 8.7 Hz, 2H), 7.57 (d, J = 8.7 Hz, 2H), 7.50 (d, J = 5.0 Hz, 1H), 7.48 (d, J = 4.9 Hz, 1H), 7.14 (t, J = 8.9 Hz, 2H), 6.65 (m, J = 17.0, 10.2 Hz, 1H), 6.34 (m, J = 17.0, 1.8 Hz, 1H), 5.80 (m, J = 10.2, 1.8 Hz, 1H). ^{13}C NMR (101 MHz, DMSO) δ 164.09, 159.04, 153.03, 151.22, 145.81, 139.97, 136.42, 135.99, 132.02, 131.59, 130.54, 128.18, 127.21, 120.55, 120.47, 119.11, 115.87, 115.65, 114.07.

4.2.24. N-(5-(4-(3-(3-(trifluoromethyl)phenyl)ureido) phenyl)pyridin-2-yl)acrylamide (VDAU7).

White solid (yield 53.1%), HRMS *m/z* calcd for $C_{22}H_{17}F_3N_4O_2$ ([M]$^+$) 426.1304, found 426.9504. m.p.=193-195°C, ^{1}H NMR (400 MHz, DMSO) δ 10.82 (s, 1H), 9.12 (s, 1H), 8.97 (s, 1H), 8.67 (d, J = 2.1 Hz, 1H), 8.28 (d, J = 8.7 Hz, 1H), 8.10 (m, J = 8.7, 2.4 Hz, 1H), 8.04 (s, 1H), 7.68 (d, J = 8.7 Hz, 2H), 7.60 (d, J = 7.4 Hz, 2H), 7.59 (s, 1H), 7.53 (t, J = 7.9 Hz, 1H), 7.33 (d, J = 7.6 Hz, 1H), 6.65 (m, J = 17.0, 10.2 Hz, 1H), 6.34 (m, J = 17.0, 1.8 Hz, 1H), 5.80 (m, J = 10.2, 1.8 Hz, 1H). ^{13}C NMR (101 MHz, DMSO) δ 164.10, 152.92, 151.27, 145.85, 141.01, 139.63, 136.04, 132.01, 131.53, 130.88, 130.39, 130.16, 129.85, 128.19, 127.23, 122.37, 119.36, 118.58, 114.66, 114.07.

4.2.25. N-(5-(4-(3-(2-chlorophenyl)ureido)phenyl)pyridin-2-yl)acrylamide (VDAU8).

White solid (yield 14.3%), HRMS *m/z* calcd for $C_{21}H_{17}ClN_4O_2$ ([M]$^+$) 392.1040, found 392.9006. m.p.=190-192°C, ^{1}H NMR (400 MHz, DMSO) δ 10.82 (s, 1H), 9.57 (s, 1H), 8.67 (d, J = 2.1 Hz, 1H), 8.36 (s, 1H), 8.28 (d, J = 8.7 Hz, 1H), 8.19 (d, J = 8.3 Hz, 1H), 8.11 (m, J = 8.7, 2.4 Hz, 1H), 7.69 (d, J = 8.6 Hz, 2H), 7.59 (d, J = 8.6 Hz, 2H), 7.50 – 7.44 (m, 1H), 7.32 (t, J = 7.8 Hz, 1H),

7.09 – 7.01 (m, 1H), 6.65 (m, J = 17.0, 10.2 Hz, 1H), 6.34 (m, J = 17.0, 1.6 Hz, 1H), 5.80 (m, J = 10.2, 1.6 Hz, 1H). ^{13}C NMR (101 MHz, DMSO) δ 164.10, 152.54, 151.27, 145.85, 139.69, 136.36, 136.03, 132.01, 131.52, 130.85, 129.71, 128.20, 128.07, 127.32, 123.86, 122.47, 121.83, 119.08, 114.08.

4.2.26. N-(5-(4-(3-(4-(trifluoromethoxy)phenyl)ureido) phenyl)pyridin-2-yl)acrylamide (VDAU9).

White solid (yield26.5%), HRMS *m/z* calcd for $C_{22}H_{17}F_3N_4O_3$ ($[M]^+$) 442.1253, found 442.9704. m.p.=220-222°C, ^{1}H NMR (400 MHz, DMSO) δ 10.81 (s, 1H), 8.94 (s, 1H), 8.89 (s, 1H), 8.66 (d, J = 2.1 Hz, 1H), 8.27 (d, J = 8.7 Hz, 1H), 8.10 (m, J = 8.7, 2.4 Hz, 1H), 7.68 (d, J = 8.7 Hz, 2H), 7.58 (d, J = 8.8 Hz, 4H), 7.30 (d, J = 8.6 Hz, 2H), 6.65 (m, J = 17.0, 10.2 Hz, 1H), 6.34 (m, J = 17.0, 1.8 Hz, 1H), 5.80 (m, J = 10.2, 1.8 Hz, 1H). ^{13}C NMR (101 MHz, DMSO) δ 164.09, 152.88, 151.25, 145.83, 143.10, 139.79, 139.42, 136.01, 132.02, 131.56, 130.72, 128.18, 127.23, 122.20, 119.93, 119.40, 119.21, 114.07.

4.2.27. N-(5-(4-(3-(2,6-dimethylphenyl)ureido)phenyl) pyridin-2-yl)acrylamide (VDAU10).

White solid (yield 35.4%), HRMS *m/z* calcd for $C_{23}H_{22}N_4O_2$ ($[M]^+$) 386.1743, found 386.9670. m.p.=290-292°C, ^{1}H NMR (400 MHz, DMSO) δ 10.81 (s, 1H), 8.97 (s, 1H), 8.65 (d, J = 2.1 Hz, 1H), 8.27 (d, J = 8.7 Hz, 1H), 8.08 (m, J = 8.7, 2.4 Hz, 1H), 7.85 (s, 1H), 7.65 (d, J = 8.7 Hz, 2H), 7.58 (d, J = 8.8 Hz, 2H), 7.08 – 7.04 (m, 3H), 6.65 (m, J = 17.0, 10.2 Hz, 1H), 6.38 – 6.30 (m, 1H), 5.80 (m, J = 10.2, 1.8 Hz, 1H), 2.23 (s, 6H). ^{13}C NMR (101 MHz, DMSO) δ 164.08, 153.57, 151.15, 145.74, 140.67, 136.04, 135.91, 135.77, 132.03, 131.68, 130.02, 128.20, 127.12, 126.44, 118.79, 114.07, 18.75.

4.2.28. N-(5-(4-(3-(3-chlorophenyl)ureido)phenyl)pyridin-2-yl)acrylamide (VDAU11).

White solid (yield 40.9%), HRMS *m/z* calcd for $C_{21}H_{17}ClN_4O_2$ ($[M]^+$) 392.1040, found 392.9001. m.p.=197-199°C, ^{1}H NMR (400 MHz, DMSO) δ 10.82 (s, 1H), 8.97 (s, 1H), 8.94 (s, 1H), 8.66 (d, J = 2.3 Hz, 1H), 8.28 (d, J = 8.7 Hz, 1H), 8.10 (m, J = 8.7, 2.4 Hz, 1H), 7.74 (s, 1H), 7.68 (d, J = 8.7 Hz, 2H), 7.58 (d, J = 8.7 Hz, 2H), 7.31 (d, J = 4.1 Hz, 1H), 7.29 (d, J = 5.6 Hz, 1H), 7.03 (m, J = 6.8, 2.2 Hz, 1H), 6.65 (m, J = 17.0, 10.2 Hz, 1H), 6.34 (m, J = 17.0, 1.8 Hz, 1H), 5.80 (m, J = 10.2, 1.8 Hz, 1H). ^{13}C NMR (101 MHz, DMSO) δ 164.10, 152.80, 151.26, 145.84, 141.69, 139.70, 136.02, 133.68, 132.02, 131.54, 130.87, 130.80, 128.18, 127.23, 121.98, 119.27, 118.08, 117.17, 114.08.

4.2.29. General procedure for the synthesis of quinazolinone diaryl urea derivatives QZAU1-5.

4.2.30. 7-Bromoquinazolin-4(3H)-one (13).

Around bottom two flask charged with 2-amino-5-bromobenzoicacid **12** (5.00 g, 23.14 mmol) was flushed with nitrogen and suspended in $HCONH_2$ (80 mL, 2.01 mmol), the mixture was stirred at 150°C for 1.5 h by atmospheric microwave heating. The product was extracted with AcOEt (50 mL ×3), washed with water, and dried over Na_2SO_4. After filtration and concentration *in vacuo*, the residue was purified by silica gel flash chromatography (PE/AcOEt=5:1) affording **13** (1.46 g, 41.24%) as white solid. mp: 259~261°C.

4.2.31. (3-(3-(4-chloro-3-(trifluoromethyl)phenyl)ureido) phenyl)boronic acid (15).

Triphosgene (0.94 g, 3.2 2mmol) was dissolved in anhydrous CH_2Cl_2 (20 mL) and the mixture was stirred on the ice-bath for 5 min. A solution of 4-chloro-3-(trifluoromethyl)aniline (1.40 g, 7.16 mmol) in anhydrous CH_2Cl_2 was added dropwise to the above mixture and stirring was continued for 15 min. Then triethanolamine (1.20 mL,17.18 mmol) diluted with CH_2Cl_2 (10 mL) was then added onto the mixture. Stirring was continued for 15 min, a solution of triethanolamine (1.20 mL, 17.18 mmol) and 3-aminophenylboronic acid 14 (0.89 g,5.73 mmol) in anhydrous CH_2Cl_2 (10 mL) was added and continued stirring for 20min. Subsequently, the ice bath was removed, and the mixture was reacted at room temperature overnight. After completion of the action, the reaction was quenched with dilute $NaHCO_3$.The organic layer was washed with water and brine, and dried overNa_2SO_4. After filtration and concentration *in vacuo*, the residue was

purified by silica gel flash chromatography (PE/AcOEt=5:1) yielding **15** as white solid (0.84 g, 32.68%).

4.2.32. 1-(4-chloro-3-(trifluoromethyl)phenyl)-3-(3-(4-oxo-3,4-dihydroquinazolin-7-yl)phenyl)urea (QZAU1).

A flask charged with $Pd(PPh_3)_4$ (0.39 g, 0.34 mmol), potassium carbonate (1.43 g, 10.35 mmol), and the key intermediate **15** (1.40 g, 3.45 mmol) and **13** (0.78 g, 3.45 mmol) were flushed with nitrogen and suspended in 1,4-dioxane (90 mL) and water (30 mL). The mixture was then refluxed overnight under nitrogen. The hot suspension was filtered and the filtrate distilled by rotary evaporation to remove 1,4-dioxane. Water (50 mL) was added and the product was extracted with AcOEt (30 mL×3), washed with water, and dried over Na_2SO_4. After filtration and concentration *in vacuo*, the residue was purified by silica gel flash chromatography (PE/AcOEt=2:1) affording **QZAU1** (0.21g) as white solid (yield 30.8%), HRMS *m/z* calcd for $C_{22}H_{14}ClF_3N_4O_2$([M+H]$^+$) 459.0757, found 459.0786. m.p. >300°C, ^{1}H NMR (400 MHz, DMSO) δ 12.30 (s, 1H), 9.26 (s, 1H), 9.02 (s, 1H), 8.21 (d, J = 8.3 Hz, 1H), 8.15 (d, J = 3.3 Hz, 1H), 8.13 (d, J = 2.4 Hz, 1H), 7.97 (s, 1H), 7.88 (d, J = 1.3 Hz, 1H), 7.80 (m, J = 8.3, 1.7 Hz, 1H), 7.68 (m, J = 8.8, 2.4 Hz, 1H), 7.61 (d, J = 8.8 Hz, 1H), 7.53 – 7.48 (m, 1H), 7.45 (d, J = 2.3 Hz, 1H), 7.44 (d, J = 1.9 Hz, 1H). ^{13}C NMR (101 MHz, DMSO) δ 161.01, 152.97, 149.75, 146.40, 146.34, 140.48, 139.83, 139.76, 132.44, 130.12, 127.16, 125.79, 125.16, 124.64, 123.64, 122.86, 122.08, 121.66, 119.29, 117.73, 117.35, 117.29.

The title compounds **QZAU2 -5** were prepared from the key intermediate **13** and **15** with a similar procedure as described for compound **QZAU1**.

4.2.33. 1-(3,5-bis(trifluoromethyl)phenyl)-3-(3-(4-oxo-3,4-dihydroquinazolin-7-yl)phenyl)urea (QZAU2).

White solid (yield 25.2%), HRMS *m/z* calcd for $C_{23}H_{14}F_6N_4O_2$ ([M+H]$^+$) 493.1021, found 493.1053. m.p. >300°C, ^{1}H NMR (400 MHz, DMSO) δ 12.30 (s, 1H), 9.49 (s, 1H), 9.16 (s, 1H), 8.21 (d, J = 8.3 Hz, 1H), 8.16 (s, 2H), 8.15 (s, 1H), 7.98 (s, 1H), 7.88 (s, 1H), 7.80 (d, J = 8.3 Hz, 1H), 7.64 (s, 1H), 7.53 (d, J = 4.1 Hz, 1H), 7.46 (s, 1H), 7.45 (s, 1H). ^{13}C NMR (101 MHz, DMSO) δ 161.01, 152.99, 149.75, 146.39, 146.30, 142.27, 140.30, 139.84, 131.33, 131.00, 130.11, 127.15, 125.80, 125.17, 125.14, 122.43, 122.09, 121.87, 119.52, 118.55, 118.52, 117.96, 114.89.

4.2.34. 1-(3-(4-oxo-3,4-dihydroquinazolin-7-yl)phenyl)-3-(3-(trifluoromethyl)phenyl)urea (QZAU3).

White solid (yield 14.4%), HRMS *m/z* calcd for $C_{22}H_{15}F_3N_4O_2$ ([M+H]$^+$) 425.1147, found 425.1176. m.p. >300°C, ^{1}H NMR (400 MHz, DMSO) δ 12.30 (s, 1H), 9.28 (s, 1H), 9.11 (s, 1H), 8.22 (d, J = 8.3 Hz, 1H), 8.15 (s, 1H), 8.05 (s, 1H), 7.98 (s, 1H), 7.88 (s, 1H), 7.81 (m, J = 8.3, 1.4 Hz, 1H), 7.62 (d, J = 8.3 Hz, 1H), 7.51 (m, J = 9.9, 7.6 Hz, 2H), 7.45 (d, J = 4.3 Hz, 1H), 7.44 (d, J = 2.1 Hz, 1H), 7.33 (d, J = 7.6 Hz, 1H). ^{13}C NMR (101 MHz, DMSO) δ 161.04, 153.12, 149.75, 146.39, 141.03, 140.66, 139.84, 130.40, 130.15, 129.84, 127.17, 126.04, 125.82, 125.16, 123.34, 122.37, 122.07, 121.51, 119.11, 118.62, 117.52, 114.64, 40.59, 40.38, 40.18, 39.97, 39.76, 39.55, 39.34.

4.2.35. 1-(3,4-difluorophenyl)-3-(3-(4-oxo-3,4-dihydroquinazolin-7-yl)phenyl)urea (QZAU4).

White solid (yield 20.2%), HRMS *m/z* calcd for $C_{21}H_{14}F_2N_4O_2$ ([M+H]$^+$) 393.1085, found 393.1125. m.p. >300°C, ^{1}H NMR (400 MHz, DMSO) δ 12.30 (s, 1H), 9.00 (s, 1H), 8.93 (s, 1H), 8.15 (d, J = 2.9 Hz, 1H), 7.96 (s, 1H), 7.87 (s, 0H), 7.80 (m, J = 8.3, 1.6 Hz, 1H), 7.70 (m, J = 13.4, 7.5, 2.6 Hz, 1H), 7.52 – 7.46 (m, 1H), 7.44 (d, J = 4.3 Hz, 1H), 7.43 (s, 1H), 7.35 (m, J = 19.6, 9.2 Hz, 1H), 7.21 – 7.13 (m, 1H). ^{13}C NMR (101 MHz, DMSO) δ 161.01, 153.03, 149.75, 146.41, 140.67, 139.81, 137.30, 137.18, 130.13, 127.15, 125.80, 125.14, 122.08, 121.45, 119.09, 117.92, 117.75, 117.52, 114.98, 107.88, 107.67.

4.2.36. 1-(3-chlorophenyl)-3-(3-(4-oxo-3,4-dihydroquinazolin-7-yl)phenyl)urea (QZAU5).

White solid (yield 25.4%), HRMS *m/z* calcd for $C_{21}H_{15}ClN_4O_2$ ([M+H]$^+$) 391.0884, found 391.0928. m.p. >300°C, ^{1}H NMR (400 MHz, DMSO) δ 12.30 (s, 1H), 9.00 (s, 1H), 8.95 (s, 1H), 8.22 (d, J = 8.3 Hz, 1H), 8.15 (s, 1H), 7.98 (s, 1H), 7.88 (d, J = 1.1 Hz, 1H), 7.80 (m, J = 8.3, 1.6 Hz, 1H), 7.75 (s, 1H), 7.52 – 7.46 (m, 1H), 7.44 (d, J = 5.0

Hz, 1H), 7.43 (s, 1H), 7.31 (s, 1H), 7.30 (s, 1H), 7.06 – 7.01 (m, 1H). ^{13}C NMR (101 MHz, DMSO) δ 161.03, 152.96, 149.76, 146.39, 141.67, 140.68, 139.82, 133.68, 130.85, 130.13, 127.16, 125.80, 125.15, 122.08, 122.01, 121.46, 119.07, 118.14, 117.50, 117.23.

4.3. Angiogenic RTK inhibition evaluation [20]

The inhibitory activity against VEGFR-2, TIE-2, and EphB4 of all the title compounds were evaluated using the ADP-Glo™ kinase assay kit (Promega, Madison) with sorafenib as positive control. The kinase assay was carried in duplicate in a reaction mixture of final volume of 10 μL. General procedures are as the following: for VEGFR-2 assays, the kinase (0.6 ng/mL) were incubated with substrates (0.2 mg/mL), title compounds (1.2×10^{-4}~12 μM) and ATP (50 μM) in a final buffer of Tris 40 mM, $MgCl_2$ 10 mM, BSA 0.1 mg/mL, DTT 1 mM in 384-well plate with the total volume of 5 μL. The assay plate was incubated at 30°C for 60 min and cooled at room temperature for 5 min, 5 μL of ADP-Glo reagent was added to stop the reaction and consume the remaining ADP within 40 min. At the end, 10 μL of kinase detection reagent was added and incubated for 30 min to produce a luminescence signal. As for TIE-2 and EphB4 assays, the kinase (2.4 ng/mL) were incubated with substrates (0.2 mg/mL), title compounds (1.2×10^{-4}~12 μM) and ATP (50 μM) in a final buffer of Tris 40 mM, $MgCl_2$ 10 mM, BSA 0.1 mg/mL, DTT 1 mM in 384-well plate with the total volume of 5 μL. The assay plate was incubated at 30°C for 4 h and cooled at room temperature for 5 min, 5 μL of ADP-Glo reagent was added to stop the reaction and consume the remaining ADP within 1 h. At the end, 10 μL of kinase detection reagent was added and incubated for 30 min to produce a luminescence signal. The luminescence was read by VICTOR-X multi- label plate reader.

4.3. Human vascular endothelial cell (EA.hy926) viability assay [21].

The viability of HUVEC (EA.hy926) was assessed using the cell counting kit-8 (CCK-8, Sigma, USA)assay according to the manufacturer's instruction. In brief, EA-hy926 cells were harvested and plated in a 96-wellplate at the density of 1×10^5 cells for each well and cultured in DMEM containing 10% FBS in humidified 5% CO_2 atmosphere. After incubation at 37 ºC for 48 h, the cells were treated with tested compounds at various concentrations for 24 h. Subsequently, premixed CCK-8 and medium (10 μL) were added into the 96-well plates to monitor cell viability and were incubated at 37 ºC for 2 h. The number of viable cells was assessed by measurement of absorbance at 450 nm by a microplate reader. The viability rate was calculated as experimental OD value/control OD value.

4.3. Cell growth inhibitory activity in cancer cell lines [22]

The antiproliferative activity of title compounds were evaluated against nine cancer cell lines. All the title compounds were evaluated using MTT assay to assess cell proliferation. Exponentially growing cells were harvested and plated in 96-well plates at a concentration of 1×10^4 cells/well, and then incubated for 24 h at 37 °C. The cells in wells were treated with title compounds respectively at various concentrations for 48 h. Then, 22 mL fresh MTT (5 mg/mL) was added to each well and incubated for 4 h at 37 °C. Supernatant was discarded, and 150 mL DMSO was added to each well. Absorbance values were determined by a microplate reader (Bio-Rad Instruments) at 490 nm. The IC_{50} values were calculated according to inhibition ratios.

4.4. Molecular docking modeling [23]

In order to understand the binding mode of inhibitors with VEGFR-2/TIE-2/EphB4, molecule docking was performed using Sybyl-X/Surflex-dock module based on the crystal structures of VEGFR-2 (PDB ID: 4ASD), TIE-2 (PDB ID: 2P4I) and EphB4 (PDB ID: 2X9F). Hydrogen was added and minimized using the Tripos force field and Pullman charges. The most potent compound (VDAU11) was depicted with the Sybyl-X/Sketch module (Tripos Inc.) and optimized applying Powell's method with the Tripos force field with convergence criterion set at 0.05 kcal/(Åmol), and assigned with the Gasteiger-Hückel charge. The docking studied was carried out using Surflex-dock module. The residues in a radius 5.0 Å around the natural ligand of VEGFR-2/TIE-2/ EphB4 in the crystal complex

were selected as the active site. Other docking parameters were kept at default.

Acknowledgments

This work was supported by the National Natural Science Foundation of China (*NSFC*, Grant No. 81573285) and the Fundamental Research Funds for the Central Universities (2015qngz13).

References

1. J.R. Nathan, G. Lakshmanan, F.M. Michael, P. Seppan, M. Ragunathan, Expression of adenosine receptors and vegf during angiogenesis and its inhibition by pentoxifylline-A study using zebrafish model, Biomed Pharmacother. 84 (2016) 1406-1418.
2. L.L. Jardim, D.R. Rios, L.O. Perucci, L.P. de Sousa, K.B. Gomes, L.M. Dusse, Is the imbalance between pro-angiogenic and anti-angiogenic factors associated with preeclampsia? Clin Chim Acta. 447 (2015) 34-38.
3. S.M. Weis, D.A. Cheresh, Tumor angiogenesis: molecular pathways and therapeutic targets, Nat Med. 17 (2011) 1359-1370.
4. D. Bouïs, Y. Kusumanto, C. Meijer, N.H. Mulder, G.A. Hospers, A review on pro- and anti-angiogenic factors as targets of clinical intervention, Pharmacol Res. 53 (2006) 89-103.
5. J.P. Himanen, K.R. Rajashankar, M. Lackmann, C.A. Cowan, M. Henkemeyer, D.B. Nikolov, Crystal structure of an Eph receptor-ephrin complex, Nature. 414 (2001) 933-938.
6. G. Aprile, M. Macerelli, F. Giuliani, Regorafenib for gastrointestinal malignancies: from preclinical data to clinical results of a novel multi-target inhibitor, BioDrugs. 27 (2013) 213-224.
7. G. Grazia, I. Penna, V. Perotti, A. Anichini, E. Tassi, Towards combinatorial targeted therapy in melanoma: from pre-clinical evidence to clinical application (review), Int J Oncol. 45 (2014) 929-949.
8. A. Temirak, M. Abdulla, M. Elhefnawi, Rational drug design for identifying novel multi-target inhibitors for hepatocellular carcinoma, Anticancer Agents Med Chem. 12 (2012) 1088-1097.
9. X. Jiang, H. Liu, Z. Song, X. Peng, Y. Ji, Q. Yao, M. Geng, J. Ai, A. Zhang, Discovery and SAR study of c-Met kinase inhibitors bearing an 3-amino-benzo[d]isoxazole or 3-aminoindazole scaffold, Bioorg Med Chem. 23 (2015) 564-578.
10. F. Ciardiello, R. Bianco, R. Caputo, R. Caputo, V. Damiano, T. Troiani, D. Melisi, F. De Vita, S. De Placido, A. R. Bianco, G. Tortora, Antitumor activity of ZD6474, a vascular endothelial growth factor receptor tyrosine kinase inhibitor, in human cancer cells with acquired resistance to antiepidermal growth factor receptor therapy, Clin Cancer Res. 10 (2004) 784-793.
11. Y.L. Chiu, D.M. Carlson, R.S. Pradhan, J.L. Ricker, Exposure-response (safety) analysis to identify linifanib dose for a Phase III study in patients with hepatocellular carcinoma, Clin Ther. 35 (2013) 1770-1777.
12. J. Zhang, Y. Zhang, S. Zhang, S. Wang, L. He, Discovery of novel taspine derivatives as antiangiogenic agents, Bioorg Med Chem Lett. 20 (2010) 718-721.
13. J. Zhang, Y. Zhang, Y. Shan, N. Li, W. Ma, L. He, Synthesis and preliminary biological evaluation of novel taspine derivatives as anticancer agents, Eur J Med Chem. 45 (2010) 2798-2805.
14. C. Wang, H. Gao, J. Dong, Y. Zhang, P. Su, Y. Shi, J. Zhang, Biphenyl derivatives incorporating urea unit as novel VEGFR-2 inhibitors: design, synthesis and biological evaluation, Bioorg Med Chem. 22 (2014) 277-284.
15. H. Gao, P. Su, Y. Shi, X. Shen, Y. Zhang, J. Dong, J. Zhang, Discovery of novel VEGFR-2 inhibitors. Part II: biphenyl urea incorporated with salicylaldoxime, Eur J Med Chem. 90 (2015) 232-240.
16. W. Lu, P. Li, Y. Shan, P. Su, J. Wang, Y. Shi, J. Zhang, Discovery of biphenyl-based VEGFR-2 inhibitors. Part 3: design, synthesis and 3D-QSAR studies, Bioorg Med Chem. 23 (2015) 1044-1054.
17. P. Su, J. Wang, Y. Shi, X. Pan, R. Shao, J. Zhang, Discovery of biphenyl-aryl ureas as novel VEGFR-2 inhibitors. Part 4: exploration of diverse hinge-binding fragments, Bioorg Med Chem. 23 (2015) 3228-3236.
18. Y. Shan, H. Gao, X. Shao, J. Wang, X. Pan, J. Zhang, Discovery of novel VEGFR-2 inhibitors. Part 5: Exploration of diverse hinge-binding fragments via core-refining approach, Eur J Med Chem. 103 (2015) 80-90.
19. S. Wang, J. Chen, Y. Fu, X. Chen, Promotion of Astragaloside IV for EA-hy926 Cell Proliferation and Angiogenic Activity via ERK1/2 Pathway, J Nanosci Nanotechnol. 15 (2015) 4239-4244.
20. H. Zegzouti, M. Zdanovskaia, K. Hsiao, S.A. Goueli, ADP-Glo: A Bioluminescent and homogeneous ADP monitoring assay for kinases, Assay Drug Dev Technol. 7 (2009) 560-572.
21. H.B. Shi, J.D. Chen, X.H. Chen, Y. He, Z.J. Yang, Effects of salvianolic acid and notoginsengtriterpenes on angiogenesis in EA-hy926 cells in vitro, Chin J Nat Med. 11 (2013) 254-257.
22. Y. Shan, C. Wang, L. Zhang, J. Wang, M. Wang, Y. Dong. Expanding the structural diversity of diarylureas as multi-target tyrosine kinase inhibitors, Bioorg Med Chem. 24 (2016) 750-758.
23. J. Zhang, Y. Shan, X. Pan, C. Wang, W. Xu, L. He. Molecular docking, 3D-QSAR studies, and in silico ADME prediction of p-aminosalicylic acid derivatives as neuraminidase inhibitors, Chem Biol Drug Des. 78 (2011) 709-717.

Table 1. Structures and RTKs inhibitory activities of title compounds (**CPMA1-11**) (IC_{50}, nM)

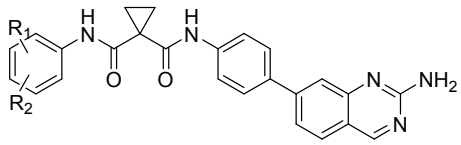

Compound	R_1	R_2	VEGFR-2	Tie-2	EphB4
CPMA1	3-CF_3	5-Br	40.37	65.26	78.92
CPMA2	2-OCF_3	4- Br	>500	>500	>500
CPMA3	2- Br	4-OCF_3	>500	>500	>500
CPMA4	2-OCF_3	5-Br	>500	>500	>500
CPMA5	2-Br	5-OCF_3	125.32	14.65	26.43
CPMA6	2-Cl	4-Cl	108.08	54.90	160.10
CPMA7	3-F	4-F	21.37	14.49	37.78
CPMA8	3-Cl	4-Cl	>500	>500	>500
CPMA9	3-CF_3	5-CF_3	>500	21.20	>500
CPMA10	3-F	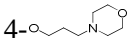	>500	>500	>500
CPMA11			>500	432.35	>500
Sorafinib			0.85	6.77	4.46

Table 2. Structures and RTKs inhibitory activities of title compounds (**VDAU1-11**) (IC_{50}, nM)

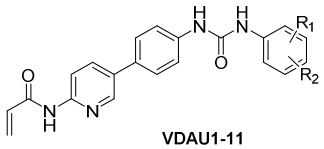

VDAU1-11

Compound	R_1	R_2	VEGFR-2	Tie-2	EphB4
VDAU1	H	4-$C(CH_3)_3$	>500	21.27	24.92
VDAU2	H	3-$CH(CH_3)_2$	2.10	9.19	23.55
VDAU3	4-Cl	3-CF_3	>500	9.77	>500
VDAU4	3-Cl	4-CH_3	>500	14.20	29.28
VDAU5	H	3-F	>500	90.86	>500
VDAU6	H	4-F	7.97	105.07	ND[a]
VDAU7	H	3-CF_3	325.82	3.59	>500
VDAU8	H	2-Cl	>500	7.97	ND
VDAU9	H	4-OCF_3	>500	59.93	ND
VDAU10	2-CH_3	6-CH_3	>500	>500	133.73
VDAU11	H	3-Cl	2.35	5.63	3.87
Soranifib			0.85	6.77	4.46

[a]ND = Not Determined.

Table 3. Structures and RTKs inhibitory activities of title compounds (**QZAU1-5**) (IC_{50}, nM)

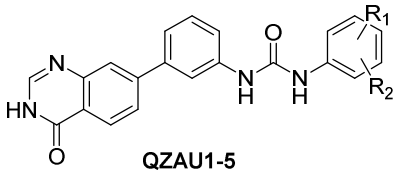

QZAU1-5

Compound	R_1	R_2	VEGFR-2	Tie-2	EphB4
QZAU1	4-Cl	3-CF_3	>500	>500	491.93
QZAU2	3-CF_3	5-CF_3	>500	245.28	>500
QZAU3	H	3-CF_3	>500	12.81	>500
QZAU4	3-F	4-F	28.95	16.55	38.52
QZAU5	H	3-Cl	34.68	24.75	47.96
Soranifib			0.85	6.77	4.46

Table 4. RTKs selectivity profile of VDAU11 (IC_{50}, nM)

Compound	VEGFR-1	VEGFR-3	EGFR	FGFR-1	FGFR-4	PDGFR-β	IGF1-R	B-Raf	c-Kit	c-Met
VDAU11	25	45	8.7	200	1076	180	40	32	68.9	57.8

Table 5. Inhibition of compounds on human vascular endothelial cell viability (IC_{50}, μM)

Compound	EA.hy 926	Compound	EA. hy926	Compound	EA. hy926
CPMA1	15.68	CPMA10	32.21	VDAU8	72.31
CPMA2	28.99	CPMA11	29.20	VDAU9	83.59
CPMA3	76.72	VDAU1	23.33	VDAU11	3.53
CPMA4	42.44	VDAU2	127.23	QZAU1	78.78
CPMA5	5.76	VDAU3	30.27	QZAU2	141.30
CPMA6	11.22	VDAU4	113.86	QZAU3	197.44
CPMA7	4.42	VDAU5	67.42	QZAU4	53.10
CPMA8	96.55	VDAU6	57.53	QZAU5	22.99
CPMA9	112.13	VDAU7	125.96	Sorafenib	24.36

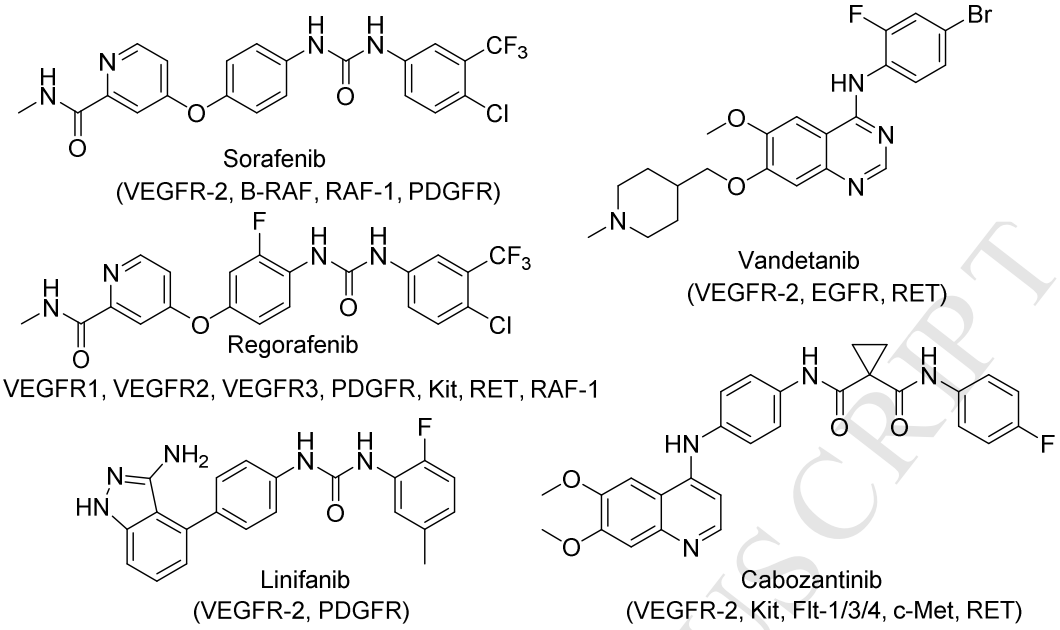

Figure 1. Multi-target RTK inhibitors currently approved or in clinical trials.

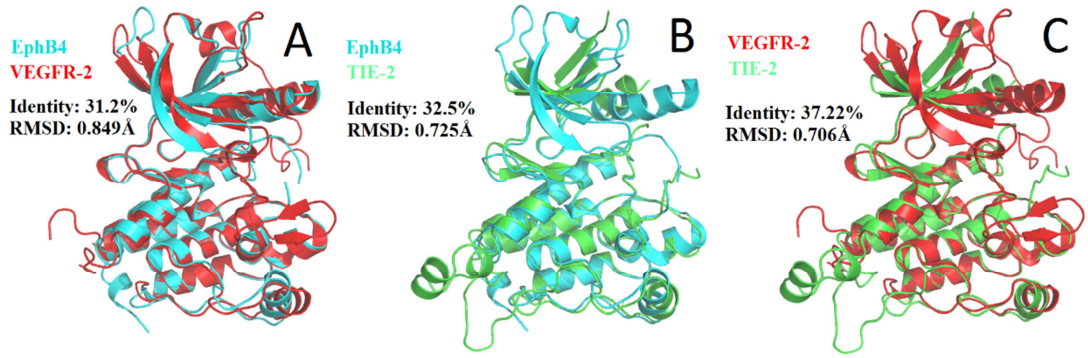

Figure 2. Protein structure alignment of three angiogenic RTKs to each other. VEGFR-2 (Red), EphB4 (Cyan), and TIE-2 (Green).

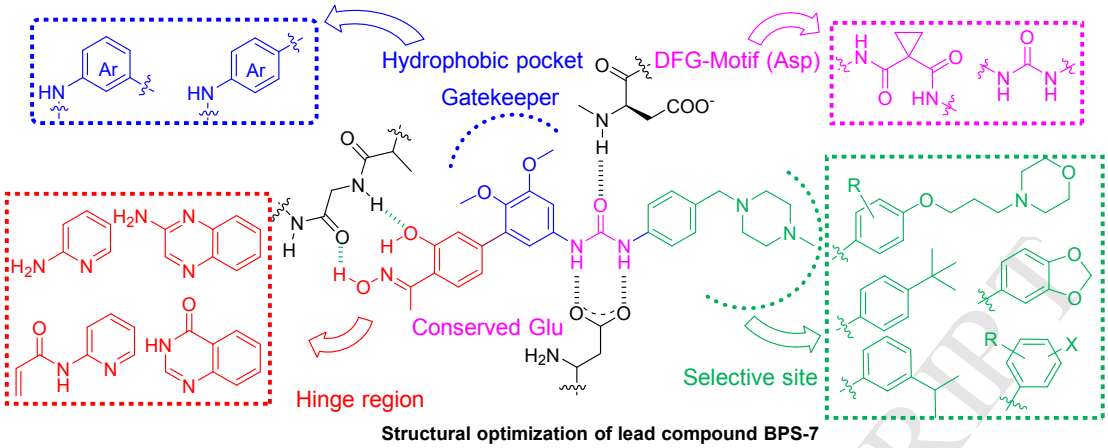

Figure 3. Design strategy and structures of novel anti-angiogenesis agents derived from BPS-7.

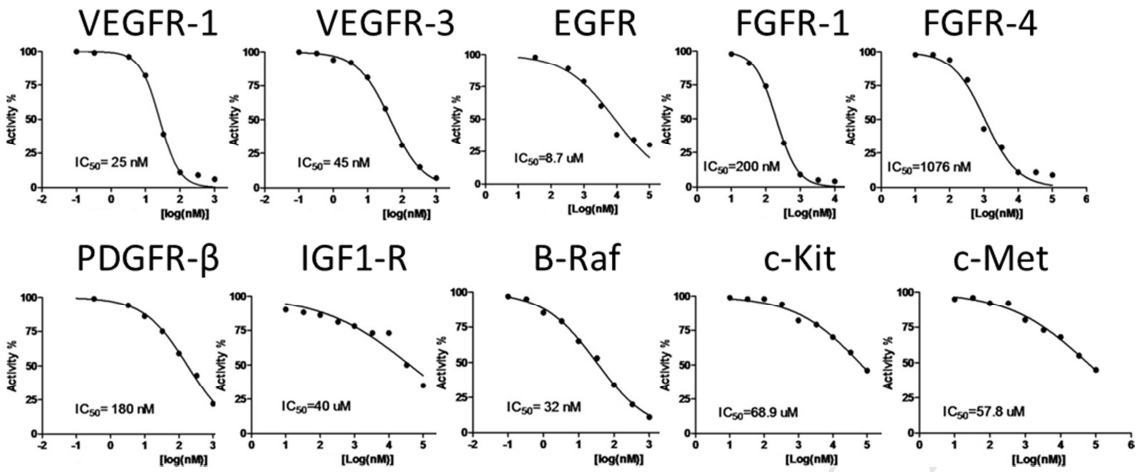

Figure 4. The selectivity of inhibitory activity of VDAU11 against various RTKs.

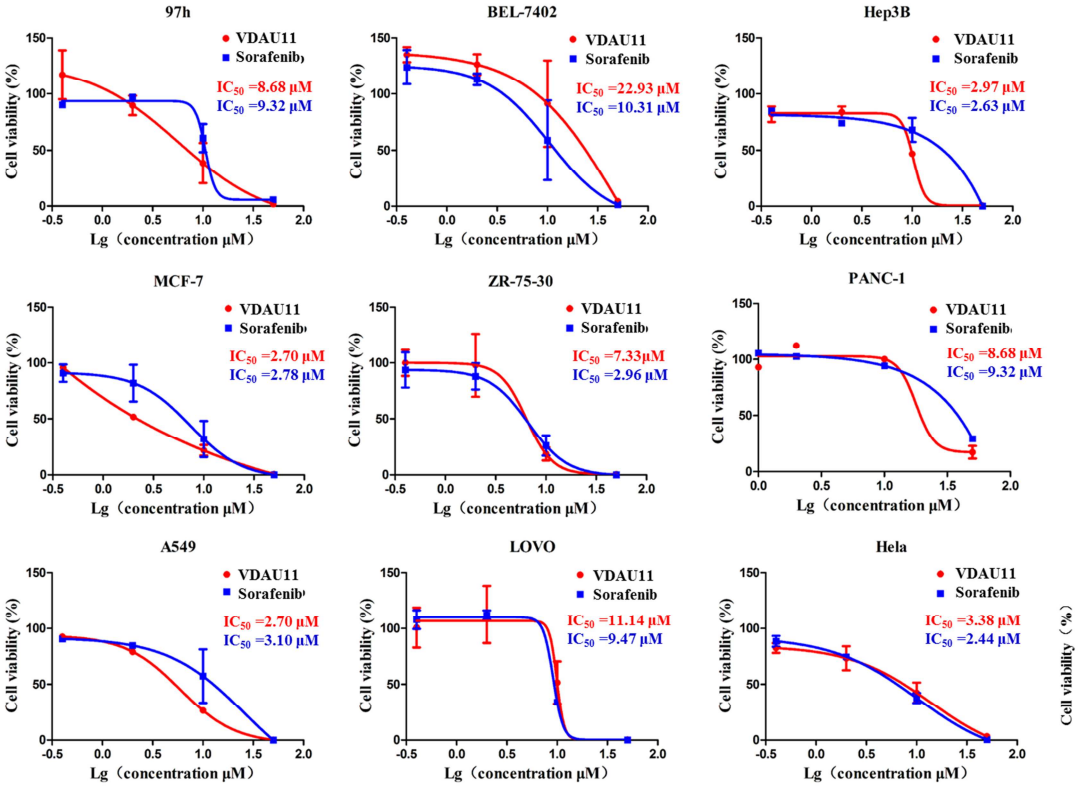

Figure 5. Inhibition of VDAU11 (Red) on the growth of nine cancer cell lines compared with sorafenib (Blue).

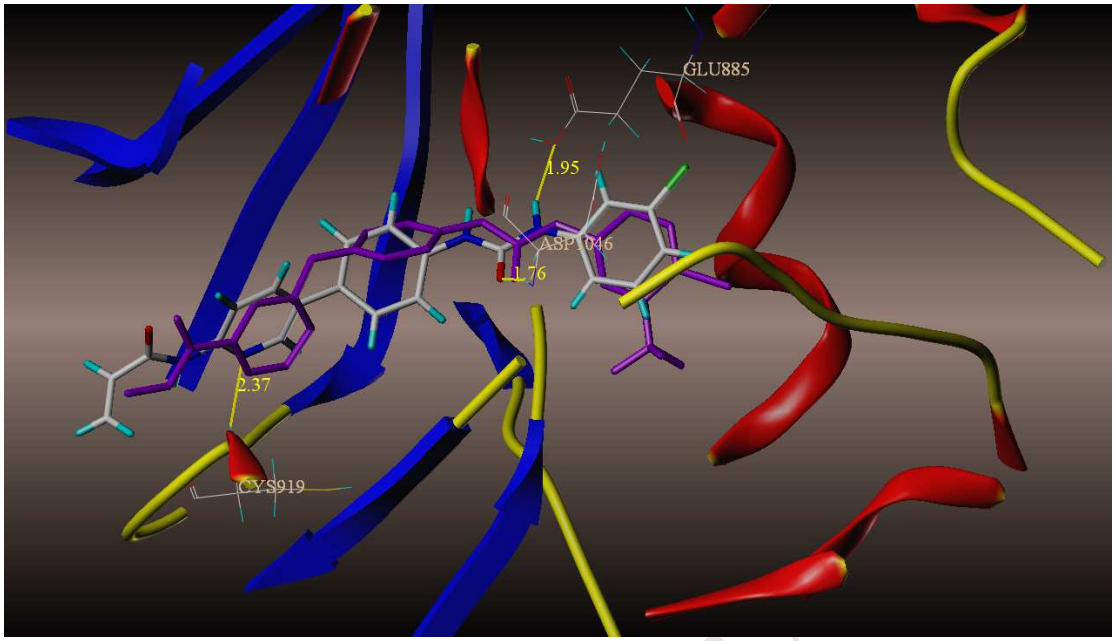

Figure 6. Docked molecule (VDAU11) and residues within 5Å in the crystal structure of VEGFR-2 (PDB ID: 4ASD).

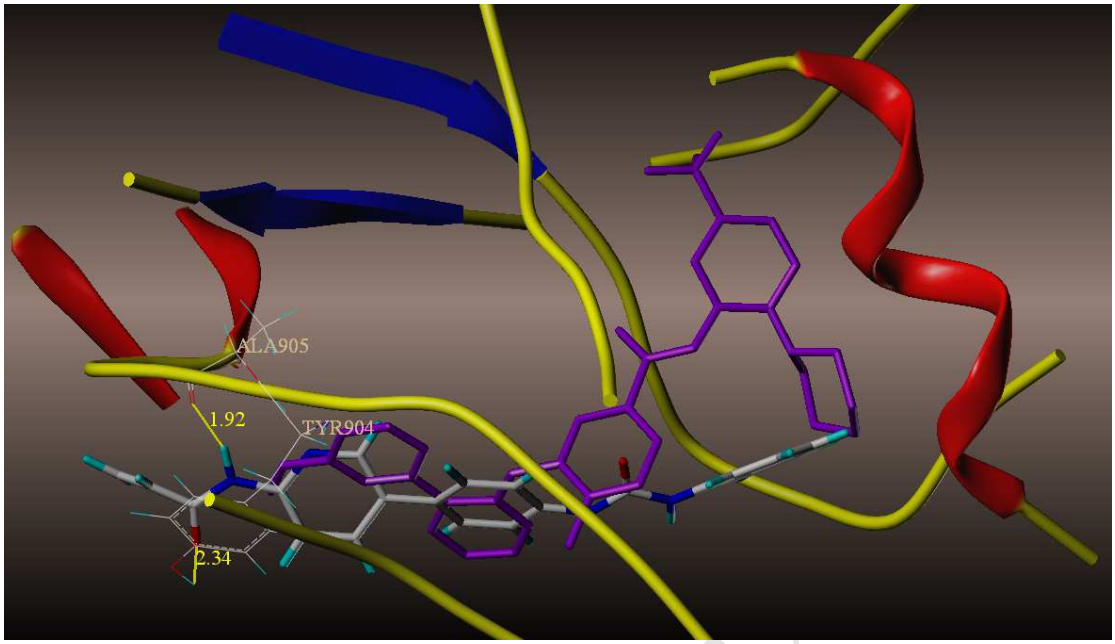

Figure 7. Docked molecule (VDAU11) and residues within 5Å in the crystal structure of Tie-2 (PDB ID: 2P4I).

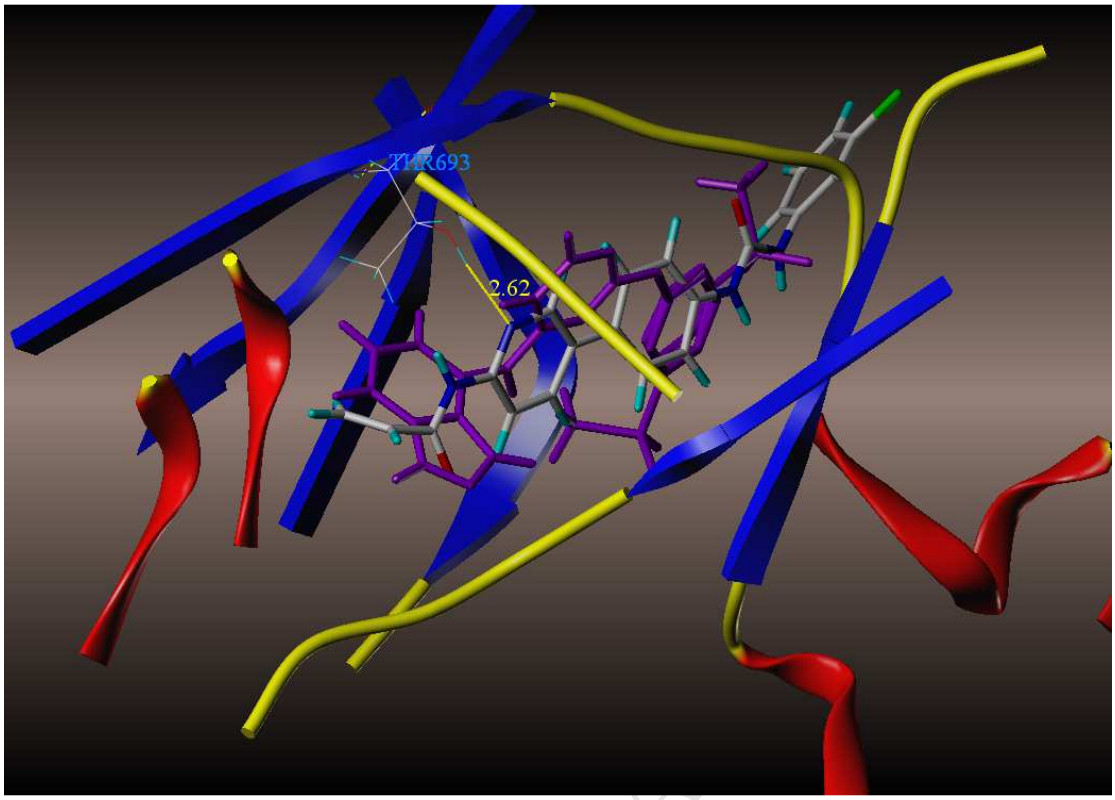

Figure 8. Docked molecule (VDAU11) and residues within 5Å in the crystal structure of EphB4 (PDB ID: 2X9F).

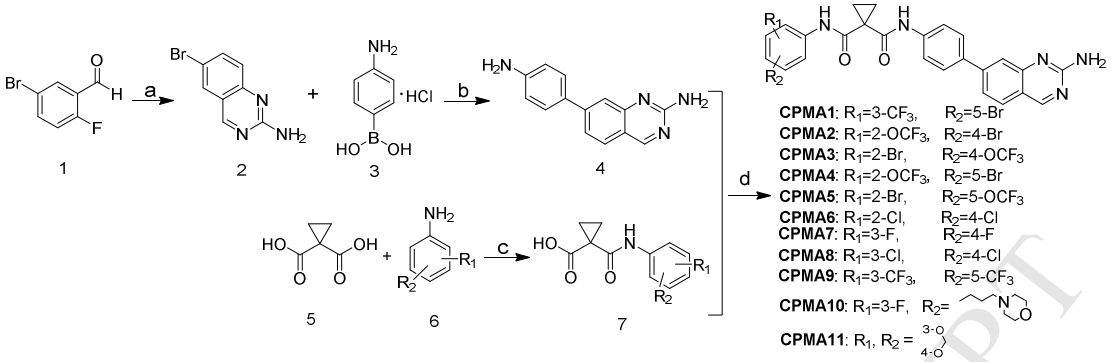

Scheme 1. Synthetic scheme of cyclopropyl-malonic amide derivatives (CPMA1-11)

Reagents and conditions: (a) guanidine carbonate, DMA, 140°C; (b) $Pd(PPh_3)_4$, Na_2CO_3, H_2O, dioxane; (c) $SOCl_2$, Et_3N, DCM; (d) HATU, Et_3N, DCM, 0°C to rt.

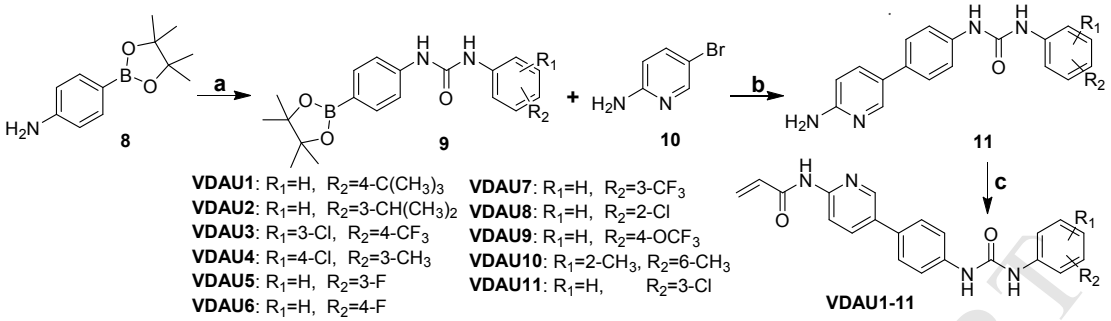

Scheme 2. Synthetic scheme of *N*-(pyridin-2-yl)acrylamidediaryl urea derivatives (VDAU1-11)

Reagents and conditions: (a) R-NH_2, BTC, Et_3N, DCM,0°C to rt; (b) $Pd(PPh_3)_4$, Cs_2CO_3, H_2O, dioxane, reflux, 100°C; (c) acryloyl chloride , Et_3N, THF, 0°C to rt.

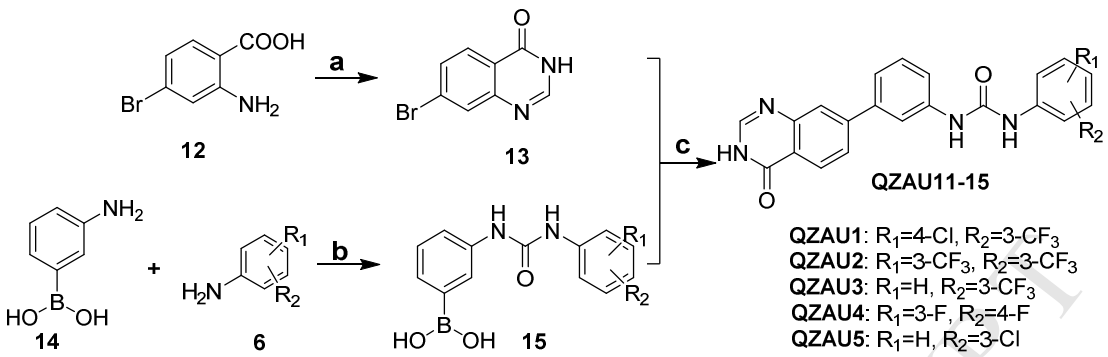

Scheme 3. Synthetic scheme of quinazolinonediaryl urea derivatives QZAU1-5

Reagents and conditions: (a) $HCONH_2$, MW, 150°C, 1.5h; (b) BTC, Et_3N, DCM, 0°C to rt; (c) $Pd(PPh_3)_4$, K_2CO_3, H_2O, CH_3CN, reflux, 100°C.

Highlights

- Structural optimization aiming at the discovery of novel anti-angiogenesis agents.
- Several compounds exhibited simultaneous inhibition against three angiogenic RTKs.
- *N*-(pyridin-2-yl)acrylamide could serve as a novel HBG of triple inhibitors.